

8-2007

# Approaches to Mitigate the Impact of Dissolved Organic Matter on the Adsorption of Synthetic Organic Contaminants by Activated Carbon

Abhishek Yadav

Clemson University, ayadav@clemson.edu

Follow this and additional works at: [https://tigerprints.clemson.edu/all\\_theses](https://tigerprints.clemson.edu/all_theses)

 Part of the [Environmental Engineering Commons](#)

---

## Recommended Citation

Yadav, Abhishek, "Approaches to Mitigate the Impact of Dissolved Organic Matter on the Adsorption of Synthetic Organic Contaminants by Activated Carbon" (2007). *All Theses*. 173.

[https://tigerprints.clemson.edu/all\\_theses/173](https://tigerprints.clemson.edu/all_theses/173)

This Thesis is brought to you for free and open access by the Theses at TigerPrints. It has been accepted for inclusion in All Theses by an authorized administrator of TigerPrints. For more information, please contact [kokeefe@clemson.edu](mailto:kokeefe@clemson.edu).

APPROACHES TO MITIGATE THE IMPACT OF DISSOLVED ORGANIC MATTER  
ON THE ADSORPTION OF SYNTHETIC ORGANIC CONTAMINANTS BY  
ACTIVATED CARBON

---

A Thesis  
Presented to  
the Graduate School of  
Clemson University

---

In Partial Fulfillment  
of the Requirements for the Degree  
Master of Science  
Environmental Engineering and Science

---

by  
Abhishek B. Yadav  
August 2007

---

Accepted by:  
Dr. Tanju Karanfil, Committee Chair  
Dr. Mark Schlautman  
Dr. Elizabeth Carraway

## ABSTRACT

The main objective of this study was to conduct a systematic investigation of various approaches to mitigate the competition of dissolved organic matter (DOM) on the adsorption of synthetic organic contaminants (SOCs) by activated carbons. TCE and atrazine were selected as the target SOCs because they are known to adsorb in different pore size regions. TCE adsorbs in the primary micropore region (i.e.,  $<10 \text{ \AA}$ ) which is inaccessible to the majority of the DOM components, while atrazine adsorbs in the secondary micropore region (i.e.,  $10\text{-}20 \text{ \AA}$ ) which is partially accessible to some DOM components. The adsorbents used in this study consisted of four activated carbons (OLC, CRC, F400He, and HD4000ST) and one activated carbon fiber (ACF: ACF10). All sorbents were basic and hydrophobic in nature and represented a set of activated carbons with gradually widening pore size distribution, from the extremely microporous carbons (ACF10 and OLC) to carbons with some amount of mesopores (CRC and F400He) and finally a predominantly mesoporous (HD4000ST) carbon.

Isotherms were performed as single solute and after preloading with a dissolved organic matter (5 mg DOC/L and 20 mg DOC/L) for both TCE and atrazine and using the five activated carbons. Single solute isotherm results showed that (i) the adsorbents with higher volume in pore sizes around the dimensions of the adsorbate molecule exhibited higher uptakes, probably due to the higher adsorption energies resulting from multiple contact points between the adsorbate molecule and the pore surface and (ii) BET surface area and total pore volume were not the primary factors controlling the adsorption. The

preloading isotherm results indicated that for TCE, the SOC adsorbing primarily in pores  $<10 \text{ \AA}$ , highly microporous GACs (i.e., activated carbons having high volumes in pores  $<10 \text{ \AA}$  and minimal volumes in pores larger than  $10 \text{ \AA}$ ) exhibited the least preloading effect and the best results for controlling DOM competition. For atrazine with optimum adsorption region in pores  $>$  than  $10 \text{ \AA}$  (i.e., partly overlapping with that of background DOM components), activated carbons with broad pore size distribution (i.e., mesoporous) or high pore volume in the optimum adsorption pore size region of atrazine (i.e.,  $10\text{-}20 \text{ \AA}$ ) showed the lowest degree of DOM preloading effect. Finally, a limited number of kinetic experiments were also carried out in this study. The mesoporous carbons demonstrated faster adsorption as compared to the microporous carbons for both TCE and atrazine in the presence or absence of background DOM.

## DEDICATION

I would like to dedicate this thesis to my parents, family, and friends and to the one and only God, who showed us the way of life in his own words of infinite wisdom in the incomparable Bhagawad Gita.



## ACKNOWLEDGEMENTS

I would like to thank Dr. Karanfil for allowing me the opportunity to work on this project as well as for his constant and thorough guidance. Dr. Karanfil is not only my advisor but also a father figure that I look up to for inspiration and have immense respect for, I could not have asked for a better mentor in my graduate school work. I would also like to thank the members of my advisory committee, Dr. Mark Schlautman and Dr. Elizabeth Carraway for their support. I am grateful to Drs. Yanping Guo and Seyed Dastgheib for being inspirational, guiding and helpful. I am also thankful to Dr. Tim DeVol for his immense patience and help in tackling the problems with the Liquid Scintillation Counter. I would like to thank Dr. Wei Cheng for his help in the adsorbent characterization, and Dr. Hochoel Song and Olivia Orr for their hard work in collecting the DOM samples at the Spartanburg R. B. Simms filtration plant. I would like to thank the National Science Foundation for funding this project

I would like to thank ‘Mama Jan’ (Jan Young) who adopted me as her ‘wayward son’ and was always there when I needed someone, both to share my joys and comfort me in my disappointments. Many thanks to all my friends in the lab, especially the folks of TKRG (Tanju Karanfil Research Group), Ilke Erdogan for being a true friend and keeping me “focused” and motivated right through, Olivia Orr for being the best friend in the world and all the wonderful memories of working together in the lab and partying all night outside (and occasionally in the lab) till the break of dawn, Sehnaz Sule for being the best and most patient roommate and friend one could ever have. Also, thanks to

Fanny Lis Ruvalcaba for being there and always taking special care of me like only she can. Finally, Miss Kathryn Ann Hanson (Kat), a wonderful person and a special friend, without whom none of this work would have been possible, she is the ‘heart’ of the research lab that keeps it alive and kicking and with whom I have wonderful memories in and outside the lab. She is one person who will forever be close to my heart.

## TABLE OF CONTENTS

|   | Page |
|---|------|
| TITLE PAGE .....  | i    |
| ABSTRACT .....  | iii  |
| DEDICATION .....  | v    |
| ACKNOWLEDGEMENTS .....  | vii  |
| LIST OF TABLES .....  | xi   |
| LIST OF FIGURES .....   | xiii |
| LIST OF SYMBOLS AND ABBREVIATIONS .....   | xvii |
| CHAPTER   |      |
| 1. INTRODUCTION .....   | 1    |
| 2. BACKGROUND .....   | 7    |
| 2.1 Activated carbons and activated carbon fibers .....   | 7    |
| 2.2 Adsorption of synthetic organic compounds by activated<br>carbons and activated carbon fibers ..... | 12   |
| 2.3 Adsorption of DOM onto activated carbons and<br>activated carbon fibers .....                       | 19   |
| 2.4 Effect of dissolved organic matter (DOM) on the<br>adsorption of SOC by activated carbon .....      | 20   |
| 3. RESEARCH OBJECTIVES .....  | 29   |
| 4. MATERIALS AND METHODS .....  | 33   |
| 4.1 Adsorbents .....  | 33   |
| 4.2 Adsorbates .....  | 34   |
| 4.3 DOM solution .....  | 36   |
| 4.4 Characterization of the adsorbents .....  | 36   |
| 4.5 Isotherm experiments .....  | 40   |
| 4.6 Kinetics experiments .....  | 41   |

## Table of Contents (Continued)

|  | Page |
|--|------|
| 5. RESULTS AND DISCUSSION.....                         | 43   |
| 5.1 Characterization of the adsorbents.....            | 43   |
| 5.2 TCE Isotherms .....                                | 49   |
| 5.3 TCE adsorption kinetics.....                       | 73   |
| 5.4 Atrazine adsorption kinetics .....                 | 80   |
| 6. CONCLUSIONS, SIGNIFICANCE AND RECOMMENDATIONS ..... | 87   |
| 6.1 Conclusions.....                                   | 87   |
| 6.2 Recommendations for future research .....          | 88   |
| APPENDIX.....  | 91   |
| REFERENCES .....                                       | 99   |

## LIST OF TABLES

| Table |  | Page |
|-------|--|------|
| 5.1   | Physicochemical characteristics of the carbons.....  | 46   |
| 5.2   | Freundlich coefficients for all TCE adsorption isotherms.....  | 58   |
| 5.3   | Reduction in TCE uptake at the two preloading conditions .....   | 62   |
| 5.4   | Freundlich coefficients for atrazine adsorption isotherms.....   | 69   |
| 5.5   | Reduction in Atrazine uptake at the two preloading condition.....  | 73   |
| A1    | Freundlich Coefficients for all TCE Adsorption Isotherms<br>along with the 95% Confidence Intervals..... | 98   |



## LIST OF FIGURES

| Figure |   | Page |
|--------|---|------|
| 2.1    | GAC and carbon fiber pore structures (Hopman et al., 1995).....           | 8    |
| 2.2    | Structure of graphite crystal (Electronics Cooling, 2007).....            | 11   |
| 4.1    | Trichloroethylene molecule.....   | 35   |
| 4.2    | Atrazine molecule.....  | 36   |
| 5.1    | Pore size distribution of all five carbons.....                           | 47   |
| 5.2    | Water vapor adsorption for all activated carbons.....                     | 48   |
| 5.3    | Single solute TCE adsorption in DDW.....                                  | 50   |
| 5.4    | TCE adsorption isotherms for carbons preloaded with 5 mg DOC/L.....       | 53   |
| 5.5    | TCE adsorption isotherms for carbons preloaded with 20 mg DOC/L.....      | 53   |
| 5.6    | Single solute DOM isotherms for all carbons.....                          | 54   |
| 5.7    | TCE single solute and preloading isotherms for OLC.....                   | 55   |
| 5.8    | TCE single solute and preloading isotherms for ACF10.....                 | 56   |
| 5.9    | TCE single solute and preloading isotherms for CRC.....                   | 56   |
| 5.10   | TCE single solute and preloading isotherms for F400He.....                | 57   |
| 5.11   | TCE single solute and preloading isotherms for HD4000ST.....              | 57   |
| 5.12   | Single solute atrazine adsorption isotherm.....                           | 64   |
| 5.13   | Atrazine adsorption isotherms for carbons preloaded with 5 mg DOC/L.....  | 64   |
| 5.14   | Atrazine adsorption isotherms for carbons preloaded with 20 mg DOC/L..... | 65   |

List of Figures (Continued)

| Figure  | Page |
|---|------|
| 5.15 Atrazine single solute and DOM preloading isotherms for OLC .....  | 66   |
| 5.16 Atrazine single solute and DOM preloading isotherms for ACF10 .....  | 67   |
| 5.17 Atrazine single solute and DOM preloading isotherms for CRC .....  | 67   |
| 5.18 Atrazine single solute and DOM preloading isotherms for F400He .....   | 68   |
| 5.19 Atrazine single solute and DOM preloading isotherms for HD4000ST .....   | 68   |
| 5.20 Single solute TCE adsorption kinetics (first 8 hours of contact time).....                                       | 75   |
| 5.21 Single solute TCE adsorption kinetics (two days of contact time).....  | 76   |
| 5.22 TCE adsorption kinetics in presence of background 5 mg DOC/L<br>(first eight hours of contact time).....         | 77   |
| 5.23 TCE adsorption kinetics in presence of background 5 mg DOC/L<br>(two days of contact time).....                  | 78   |
| 5.24 OLC kinetics for TCE adsorption (two days of contact time).....  | 78   |
| 5.25 CRC kinetics for TCE adsorption (two days of contact time).....  | 79   |
| 5.26 F400He kinetics for TCE adsorption (two days of contact time).....   | 79   |
| 5.27 HD4000ST kinetics for TCE adsorption (two days of contact time).....   | 80   |
| 5.28 Single solute atrazine adsorption kinetics (twelve hours of contact time).....                                   | 81   |
| 5.29 Single solute atrazine adsorption kinetics (two days of contact time).....                                       | 82   |
| 5.30 Atrazine adsorption kinetics in the presence of 5 mg DOC/L<br>background DOM (twelve hours of contact time)..... | 83   |
| 5.31 OLC adsorption kinetics for atrazine (two days of contact time).....   | 84   |
| 5.32 CRC adsorption kinetics for atrazine (two days of contact time).....   | 84   |
| 5.33 F400He adsorption kinetics for atrazine (two days of contact time).....  | 85   |

List of Figures (Continued)

| Figure  | Page |
|---|------|
| 5.34 HD4000ST adsorption kinetics for atrazine (two days of contact time) .....   | 85   |
| A1 TCE adsorption isotherms in DDW normalized by volume available<br>in 5-8 Å pore size region.....   | 92   |
| A2 TCE adsorption for carbons preloaded by 5 mg/L DOM normalized<br>by volume available in 5-8 Å pore size region .....                           | 93   |
| A3 TCE adsorption for carbons preloaded with 20 mg/L DOM<br>normalized by volume available in 5-8 Å pore<br>size region .....                     | 94   |
| A4 Atrazine adsorption isotherms for all carbons in DDW normalized<br>by volume available in 10-20 Å pore size range.....                         | 95   |
| A5 Atrazine adsorption isotherms for all carbons preloaded<br>with 5 mg/L DOM normalized by volume<br>available in 10-20 Å pore size region ..... | 96   |
| A6 Atrazine adsorption isotherms for all carbons preloaded with<br>20 mg/L DOM normalized by volume available<br>in 10-20 Å pore size region..... | 97   |



## LIST OF SYMBOLS AND ABBREVIATIONS

### Greek Symbols

$\pi$  Pi

### Abbreviations

|                   |   |
|-------------------|---|
| ACF               | Activated Carbon Fiber                            |
| BET               | Brunauer-Emmett-Teller equation                   |
| C                 | Elemental Carbon                                  |
| CO <sub>2</sub>   | Carbon dioxide                                    |
| DFT               | Density Functional Theory                         |
| GAC               | Granular Activated Carbon                         |
| H-bonding         | Hydrogen bonding                                  |
| HCl               | Hydrochloric acid                                 |
| IUPAC             | International Union of Pure and Applied Chemistry |
| N                 | Elemental Nitrogen                                |
| NaOH              | Sodium Hydroxide                                  |
| PAC               | Powdered Activated Carbon                         |
| pH                | $-\log\{H^+\}$                                    |
| pH <sub>pzc</sub> | pH of point of zero charge                        |

List of Symbols and Abbreviations (Continued)

|                    |   |
|--------------------|---|
| PSD                | Pore Size Distribution                        |
| SEC                | Size Exclusion Chromatography                 |
| SOC                | Synthetic Organic Chemical                    |
| USEPA              | United States Environmental Protection Agency |
| $V_{\text{micro}}$ | micropore volume                              |
| $V_{\text{total}}$ | total pore volume                             |

## CHAPTER 1

### INTRODUCTION

Large numbers of synthetic organic compounds (SOCs) have been produced for various industrial and domestic uses. Some of these compounds and their process by-products have been found to be toxic, carcinogenic, mutagenic or teratogenic. Since SOCs have entered water sources as a result of accidental or intentional releases, and/or insufficient treatment, the Clean Water Act and its amendments have been promulgated by United States Environmental Protection Agency (USEPA) (USEPA, 1995). Later, the Safe Drinking Water Act and its amendments have been passed to protect the public from exposure to some of these undesirable and harmful chemicals (USEPA, 2007). Currently, 53 SOCs are classified as priority pollutants and regulated by the USEPA.

The USEPA has designated activated carbon adsorption as one of the “Best Available Technologies” to remove SOCs from aqueous solutions (Safe Drinking Water Act Amendments of 1986; Pointus, 1996a, 1996b). Activated carbon is a porous sorbent with high degree of porosity and extensive internal surface area (e.g., 800-1000 m<sup>2</sup>/g). It can be produced from a variety of carbonaceous materials including wood, coal, lignite and coconut shells. The carbon basal planes, heterogeneous surface functional groups, and various inorganic components constitute the skeleton of activated carbon. Overall, the characteristics of activated carbon (surface area, pore size distribution, and surface chemistry) and adsorbate (molecular size, molecular structure (e.g., the presence of functional groups)), and the background solution chemistry (pH, adsorbate concentration,

presence of competitive solutes, ionic strength) all affect the adsorption of SOC by activated carbons. The pore size distribution of activated carbon with respect to the size of SOC molecules is important for adsorption. Depending on the molecular dimensions of target SOC, there is an optimum carbon pore size region that maximizes the uptake of the SOC due to enhanced adsorption in this region.

Natural organic matter (NOM), a heterogeneous mixture of complex organic compounds including humic substances, hydrophilic acids, proteins, lipids, carboxylic acids, polysaccharides, amino acids, and hydrocarbons (Thurman, 1985; Croue et al., 2003), is ubiquitous in fresh waters. The dissolved components of NOM (i.e., DOM: the portion of NOM passes through a 0.45  $\mu\text{m}$  filter) constitute the most problematic fraction of NOM with regard to drinking water treatment and supply, since they are partly removed from water by conventional treatment processes. The DOM interferes with the adsorption of SOC through either direct competition for the adsorption sites or blocking the entrance of some carbon pores for SOC adsorption. It has been shown that DOM molecules cannot access pores less than 10  $\text{\AA}$  and are generally adsorbed in pores with size ranging from 10-30  $\text{\AA}$  (Pelekani and Snoeyink, 2000; Quinlivan et al., 2005). This is also consistent with another study that reported the approximate diameters of aquatic DOM in the range of 10 to 17  $\text{\AA}$  (Moore et al., 2001)

After conducting a series of experiments with atrazine adsorbing in the 8-20  $\text{\AA}$  pore size region, which is also accessible to some DOM components, Pelekani and Snoeyink (2000) proposed that one method to mitigate the DOM-SOC competition is to use an activated carbon with broad pore size distribution and sufficient pore volumes in

the optimum adsorption pore size regions of both target SOC and DOM. However, in a separate study it was shown that for a SOC adsorbing in pores less than 10 Å (e.g., TCE), the carbons with wide pore size distribution performed poorly as compared to carbons that were extremely microporous with most of pore volume in pores less than 10 Å, a region inaccessible to the DOM molecules (Karanfil et. al, 2006). It was also demonstrated that for SOC molecules that adsorb in the micropore region inaccessible to DOM molecules, the best way to reduce the competitive effect of DOM was to use a microporous carbon adsorbent with almost all of volume in pores less than 10 Å. These microporous carbons appear to act as molecular sieves to separate the target SOC molecule from the DOM containing aqueous solution (Karanfil et al., 2006).

Considering these findings, it was hypothesized in this study that 10 Å represents an important cutoff value for developing strategies to minimize the impact of DOM on SOC adsorption. It was postulated that for the adsorption of SOC with target adsorption region in pores less than <10 Å (e.g., TCE), one possibility to mitigate the DOM competition is to use a very microporous activated carbon having mainly pores <10 Å, which are accessible to the SOC but not the DOM components. In this case, the activated carbon is expected to act as a molecular sieve to minimize the competition of the DOM molecules, as long as they do not completely block the pathway of the SOC molecules to their adsorption pores. The second possibility is to use an activated carbon with a broad pore size distribution including appreciable pore volumes in both transitional pores (i.e., secondary micropores (10-20 Å) and mesopores (20-50 Å)) to accommodate DOM molecules and primary micropores (i.e., <10 Å) for the target SOC (e.g., TCE). It was

further postulated that if the optimum adsorption region of the SOC is pores  $>10 \text{ \AA}$  (i.e., the optimum adsorption pore regions of target SOC and some DOM components overlap (e.g., atrazine)), then activated carbons with high pore volumes in the secondary micropores and mesopores should be selected to reduce the DOM competition.

The main objective of this study was to conduct a systematic experimental investigation to test these proposed hypotheses and to determine the approaches to mitigate DOM competition on the SOC adsorption. Two SOCs adsorbing in the significantly different pore size regions, TCE and atrazine, were selected as the target compounds. Although the adsorption of these two compounds has been individually investigated in several studies (Karanfil and Dastgheib, 2004, 2006; Pelekani and Snoeyink, 1999, 2000, 2001), their adsorption on the same set of adsorbents with different pore size distributions in the presence of the same background DOM has not been investigated and compared side by side. Since the hypotheses postulated above are mainly derived from the adsorption results of carbon fibers, and it is known that activated carbon fibers and activated carbons have important differences in their pore structures, four GACs were selected for this study to examine the proposed hypotheses for GAC applications. One ACF was also included in the adsorbent matrix for the purpose of comparing the results between GACs and ACFs. The selected adsorbents covered a wide and gradually increasing pore size distribution, ranging from very microporous to some degree of mesoporous and finally to a predominantly mesoporous. These adsorbents were selected because they had also relatively similar surface acidity and hydrophobicity. Similar surface chemistry was an important consideration in the adsorbent selection

because the main goal of this study was to obtain a better understanding on the interplay between the optimum adsorption pore size regions of the target SOC and the DOM controlling the SOC-DOM competitive adsorption.

Furthermore, in practical applications, adsorption kinetics usually is of equal if not greater importance than adsorption equilibrium. However, very few studies were performed to investigate the effect of NOM competition on the adsorption kinetics of micropollutants on carbonaceous adsorbents. Therefore, another objective of this study was to provide some preliminary kinetic information on the DOM-SOC competitive adsorption. This was conducted by comparing the single solute adsorption kinetics of each individual SOC on the four GACs with that obtained in solution containing background DOM of concentration typically encountered in the treatment plants. These investigations, in conjunction with the equilibrium studies are intended to provide a better mechanistic understanding of the SOC-DOM competitive adsorption on activated carbons and providing some guidelines for selecting appropriate activated carbons in practical applications.



## CHAPTER 2

### BACKGROUND

#### 2.1 Activated carbons and activated carbon fibers

Granular activated carbon (GAC) and powdered activated carbon (PAC) have been used to remove a wide range of priority organic pollutants from water and wastewater. The difference between GAC and PAC is that the GAC are irregular shaped particles with commercially available sizes ranging from 0.2 to 5 mm, while PAC is pulverized form of GAC with a size predominantly less than 0.18 mm (US Mesh 80) (Karanfil, 2006). The precursors of GAC and PAC are carbonaceous materials such as bituminous coal, lignite, coconut shells, or wood.

Activated carbon fibers (ACFs) are prepared from homogenous polymeric-based materials such as polyacrylonitrile, cellulose, pitch or other non heterocyclic aromatic precursor. ACFs display a number of advantages over GAC PAC. The fibers in addition to being more chemically stable are also significantly more heat resistant than GAC. The lower ash and higher carbon contents make ACFs more hydrophobic than GACs and PACs. ACFs have uniformly sized, slit shaped pores oriented along the longitudinal axis (Kaneko et al., 1993) (Figure 2.1). The advantage of having sharp pore size distribution is that the transition pathway from the larger mesopore opening on the surface to the micropores located in the bulk of the fibers is short, which is reported to lead to faster sorption kinetics as compared to GACs and PACs (Kasaoka et al., 1989a; Hopman et al., 1995). ACFs demonstrate greatly enhanced adsorption of SOCs in the gas phase

compared to GAC and PAC of comparable surface area (Economy et al., 1992; Dimotakis et al., 1995). In addition, ACFs are commercially available as fiber cloth; consequently it is convenient to incorporate them into the existing treatment systems by immersion into tanks or pipes. However, the major drawback preventing the widespread application of ACFs in water and wastewater treatment has been their relatively high cost. The price of ACF can cost as much as \$100 per pound, whereas GAC is comparatively cheaper at only around \$1 per pound (Mangun et al., 2001).

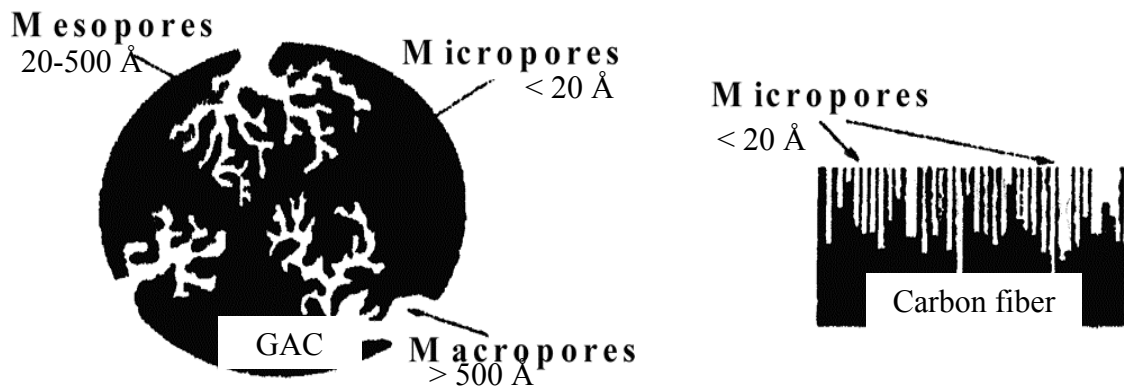


Figure 2.1 Illustration of GAC and carbon fiber pore structures (Hopman et al., 1995)

### 2.1.1 Activated carbon and carbon fiber production

Any carbonaceous material can be converted to activated carbon due to the fact that activated carbon is structurally a non-graphitic carbonaceous material. The most common precursors of activated carbon production are wood, coconut shell, fruit seeds, coals, lignite, and petroleum coke. These are materials with high carbon content, low

inorganic contents, and relatively inexpensive. The precursor and the activation conditions determine the properties of the final activated carbon products.

The methods of activated carbon production can be classified into two categories:

(i) Thermal Activation (or physical activation)

(ii) Chemical Activation

Thermal activation usually consists of two steps: the carbonization of the raw material followed by the activation process. Carbonization is the pyrolytic decomposition of precursor in the presence of an inert gas (e.g., nitrogen). This step produces char rich in carbon. In the activation process, the remaining char is partially gasified by an oxidizing agent (e.g. steam) in direct fired furnaces. When both these steps are carried out simultaneously, the process is called as direct activation.

Chemical activation is a single step carbonization process. The precursor is impregnated with significant amounts of activation agent then heated at high temperatures. Some of the commonly used chemical agents are phosphoric acid, zinc chloride, and alkali chemicals (Weber and Van Vliet, 1972). The commonly used chemical reagent to precursor weight ratio is around 1:4. After the carbonization process, the material remaining is thoroughly washed to eliminate any excess chemical agent.

Chemical activation can almost completely remove the heteroatoms like hydrogen and oxygen at a lower temperature compared to that of physical activation (Jankowska et al., 1991). Additionally, the carbon product yield of chemical activation is higher than that of physical activation due to low activation temperature and cross linking reactions caused by activation agent. Thus the compounds that would otherwise volatilize in

physical activation due to the high temperature will stay bound (Jagtoyen et al., 1992; Jagtoyen et al., 1993 and Solum et al., 1995).

The starting materials for the manufacture of ACFs are cross-linked fibers (novoloid fibers). These fibers are infusible and insoluble and have very high resistance to chemical attack (Hayes, 1985). Novoloid fibers are carbonized and activated with a one step process to produce ACF. The surface area, pore volume, and mean pore size of final ACF will increase with the increase of activation time (Hayes, 1985), which makes it possible to tailor the level of activation of the fibers for the optimal adsorption of a particular compound.

ACFs are produced by gradually heating the novoloid fibers to 900°C in the atmosphere of steam and/or carbon dioxide. This may be either a batch or continuous process. Specific surface areas as high as 2500 m<sup>2</sup>/g may be obtained, but due to increased costs and diminished yields, ACFs with specific surface areas of 1500 or 2000m<sup>2</sup>/g are usually the practical limit for most purposes (Hayes, 1985).

### 2.1.2 The structure of activated carbon and carbon fiber

The large surface area of activated carbon is almost exclusively within the particles. Structurally, activated carbon is considered to be made up of clusters (microcrystallites). These microcrystallites are rigidly interconnected and are made up of a stack of graphitic planes. Every carbon atom present within one particular plane is joined to three adjacent carbon atoms in the same plan by  $\sigma$  bonds. The fourth carbon atom participates in through  $\pi$  bond (Figure 2.2).

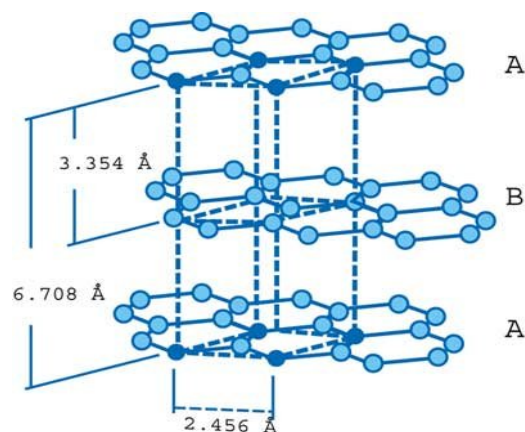


Figure 2.2 Structure of graphite crystal (Electronics Cooling, 2007)

The basal planes of the microcrystallites exposed within the micropore fissures during activation constitute the intraparticle surface of the activated carbon. Primarily the edges of the graphitic planes comprise the sides of the microcrystallites. The microcrystallite is estimated to be a stack of 5-15 layers of graphitic planes giving it a diameter or height of about 2-5 nm (Wolff, 1959; Snoeyink and Weber, 1967). Selective oxidation of inter-microcrystallite material gives rise to an extensive network of macropores, mesopores and micropores. The fissures within and parallel to the graphitic planes are considered to be micropores, whereas the channels through the graphitic regions and interstices between microcrystallites are considered to be macropores (Weber, 1972).

The carbon matrix contains several heteroatoms (oxygen, hydrogen, and nitrogen) either in the form of single atom and/or functional groups (Snoeyink and Weber, 1967; Pan and Jaroniec, 1996). The carbon basal planes, surface functional groups (mainly

oxygen containing), and inorganic impurities constitute the heterogeneous surface of the activated carbon (Puri, 1970).

The pores in ACF are small and uniform in nature. The nature of the precursor and the graphitic character of the ACFs make the pore size distribution very narrow and uniform. Also, the precursor material is responsible for the nearly ash-free nature of ACFs. Both ACF and GAC have graphitic structure in which the graphene sheets are spaced at approximately 3.35 Å (Figure 2.2). The carbon atoms at the edges of the basal planes are active sites for gasification (the zigzag edges are more active than the arm chair edges), whereas those on the basal planes are not (Yang, 1984; Yang and Duan, 1985). In the case of ACFs, once initiated, the gasification will continue to the neighboring edge sites along the same graphene sheet creating pores that are confined within two graphene sheets. Consequently the pores are approximately 7-10 Å in size and elongated within two graphene sheets. If desired, the pore size and the pore size distribution in the ACF can be tailored by adding a catalyst before activation (Freeman et al., 1989).

## 2.2 Adsorption of synthetic organic compounds by activated carbons and activated carbon fibers

Adsorption of small molecular weight SOC by activated carbons from aqueous solution is generally controlled by three types of interactions: i) SOC-activated carbon, ii) SOC-water and iii) activated carbon-water (Karanfil and Dastgheib, 2004). These interactions are discussed in detail in the following sections.

### 2.2 .1 SOC-activated carbon interaction

The SOC-activated carbon interaction is influenced by three factors: namely, the physicochemical properties of the activated carbon, the molecular structure of the SOC, and the solution chemistry. The type of interactions occurring between the carbon surface and the adsorbates can be physical interactions, chemical interactions or electrostatic interactions. (Lee et al., 1981; Weber et al., 1982; Summers and Roberts 1988a, b; Radovic et al., 1997; Newcombe and Drikas, 1997; Newcombe et al., 1997; Karanfil et al., 1998).

In physical adsorption (physisorption), the electrons maintain their association with the original nuclei, whereas in chemical adsorption (chemisorption) there is a transfer and/or sharing of electrons between the adsorbate molecules and the carbon surface. A third type of interaction, electrostatic interaction, occurs between adsorbate ions and charged functional groups on the carbon surface (Weber and Van Vliet, 1980).

#### 2.2.1.1 Physisorption

Physisorption occurs through non-specific interactions existing between any kind of molecules, irrespective of the chemical structures. These type of non-specific interactions are generally referred to as van der Waals forces. These are a superposition of three types components, namely, London dispersive energies, Debye energies, and Keesom energies. consisting of London dispersion forces and classical electrostatic forces (Weber and Van Vliet, 1980). The most important physical factor influencing the adsorption of SOC onto activated carbons is the carbon pore size distribution.

#### 2.2.1.1.1 Non-specific van der Waals interactions

The origin of London dispersive energies is due to the time-varying, uneven electron distributions in adjacent molecules. The intensity of such unevenness in a particular molecule is related to its ability to be polarized. Consequently, the intensity of intermolecular attraction energies arising from these time-varying dipoles is related to the product of the polarizabilities of each of the interacting set of atoms

Debye energies are a result of the dipole-induced dipole interactions. Juxtaposition of atoms with different electronegativities causes dipoles within chemical structures. Juxtaposition such a permanent dipole moment in one chemical to material with a time-averaged even electron distribution causes the formation of an uneven electron distribution in the second material. The resultant intermolecular attraction has strength proportional to the product of the dipole moment of the first molecule the polarizability of the second molecule.

Keesom energies result from dipole-dipole interactions. Permanent dipoles in each substance causes the molecules to orient in such a manner that the dipoles are oriented in a head-to-tail manner. The overall strength of these interactions is proportional to the product of the dipole moments of the two interacting molecules and the orientation of the interacting molecules.

#### 2.2.1.1.2 Effect of activated carbon pore size distribution on SOC adsorption

Pore size has been classified by the International Union of Pure and Applied Chemistry (IUPAC) according to pore diameter into four types: macropores ( $> 500 \text{ \AA}$ ), mesopores ( $20\text{-}500 \text{ \AA}$ ), secondary or supermicropores ( $7\text{-}20 \text{ \AA}$ ), and primary or ultramicropores ( $< 7 \text{ \AA}$ ) (Lastoskie et al., 1993). The adsorption process is highly influenced by the pore size distribution (PSD) of the adsorbent. As the pore width approaches the adsorbate dimensions, multiple contact points develop between the adsorbate molecule and the surface of the adsorbent. These surface forces overlap leading to stronger adsorption or higher adsorption energy which consequently enhances the adsorption of SOC by the microporous activated carbons (Economy et al., 1992 and Dimotakis et al., 1995). This is referred to as the ‘overlapping potential effect’. The adsorption energy is greater in micropores and hence increasing the microporosity would increase the adsorption of low molecular weight SOC molecules (Everett and Powl, 1976); Greg and Sing, 1982; Cal et al., 1994). In a recent study performed by Karanfil and Dastgheib (2004), it was demonstrated that the adsorption of trichloroethylene (TCE) by fibrous and granular activated carbons increased as the pore volume in the micropore region of  $<10 \text{ \AA}$  increased. Their results indicated that due to the flat orientation of the TCE molecule, it was able to diffuse into the deep regions of the carbon micropore (Karanfil and Dasgtheib, 2004). Kasaoka et al., (1989a and 1989b) reported that the uptake of SOC by microporous carbons occurred only in pores about 1.7 times larger than the second widest dimensions of the adsorbate molecules.

In gas phase adsorption studies, adsorption of butane by ACFs with different pore size distributions showed a crossover regime (Foster et al., 1992). At low butane pressures, the ACF with lowest surface area and smallest pore sizes exhibited the highest uptake, whereas at high pressures the ACFs with highest surface area and largest pore size and volume had highest adsorption capacities. The researchers explained that at low concentrations butane molecules adsorbed more tightly and condensed in the smaller pores; as a result the ACFs with the least pore volume demonstrated highest adsorption. At higher concentrations, the pore volume becomes the limiting factor. Hence the ACF with highest surface area and pore volume demonstrated highest adsorption merely due to the larger available pore volume. The adsorption of acetone by ACFs of different pore sizes also demonstrated a similar crossover regime (Mangun et al., 1999).

#### 2.2.1.2 Chemisorption

Chemisorption occurs when the affinity between the solute and the carbon surface is significant and as a result the molecular orbitals overlap in the respective phases. This leads to a transfer and share of electrons between the solute and adsorbent, localized at the active centers on the adsorbent (i.e., the basal planes, unpaired electrons at the edges of the terminated basal planes and/or the surface functional groups). Chemical interactions are stronger than physical interactions, and are favored at higher temperatures. Physisorption, on the other hand, increases with decreasing temperatures (Weber and Van Vliet, 1980). Some of the examples of chemisorption include electron donor-acceptor interaction between the carbonyl oxygen on the carbon surface (donor)

and the electron deficient aromatic ring of the solute (acceptor) and the H-bonding between the oxygen-containing surface functional groups (carboxylic and hydroxyl groups) and the solute (Weber and Van Vliet, 1980).

### 2.2.1.3 Electrostatic interactions

The third category of SOC-activated carbon interactions is the electrostatic interactions between ionic SOC and the charged functional groups on the carbon surface. The weak organic acids and bases dissociate in solution. The degree of dissociation depends upon the magnitude of the difference between the  $pK_a$  of the SOC molecules and the pH of the solution. In addition, the surface of the carbon carries a net positive or negative charge depending upon the pH of the solution and the pH of the point of zero charge ( $pH_{pzc}$ ) of the carbon. If the pH of the media is higher than the  $pH_{pzc}$ , the surface will collect net negative charge. Conversely, if the pH is lower than  $pH_{pzc}$ , the surface will carry a net positive charge. Therefore, there will be either electrostatic attraction or repulsion between the carbon surface and the ionizable SOC depending on the pH of the media,  $pK_a$  of the SOC molecules, and  $pH_{pzc}$  of the activated carbon.

### 2.2.2 SOC-water interaction

The SOC-water interaction relates primarily to the chemical compatibility between SOC molecules and water. The driving force for SOC molecules to escape to the interfaces between solvent and adsorbent surface increases with the increasing hydrophobicity of the SOC. This is referred to as “Solvent Motivated Adsorption,” an

important phenomenon in the adsorption of SOC from aqueous solution by activated carbons because a significant portion of the activated carbon surface is nonpolar and hydrophobic. According to Lundelius' Rule, as the solubility of the SOC decreases the extent of adsorption by activated carbon increases (Ross and Morrison, 1988). The solubility of an organic compound decreases as the chain length of organic subunits increases and hence the adsorption increase as the homologous series is ascended (Weber, 1972). It is noteworthy that these rules are valid only in the absence of the size exclusion effect which limits the access of adsorbate molecules to the deeper region of carbon pores.

As the polarity increases, the solubility of the SOC increases and consequently its adsorption by activated carbon decreases. The polarity of SOC molecules can result from the difference in the electronegativities among the various atoms, which causes an unequal distribution of electron density, or due to the presence of various functional groups. Also, ions are more soluble in water compared to their neutral molecules and hence generally the undissociated SOC molecules adsorb more strongly than their ionized forms.

### 2.2.3 Activated carbon-water interaction

The activated carbon-water interaction depends on the polarity of the carbon surface which results from the hydrophilic surface sites. Water molecules adsorb on these hydrophilic sites to form clusters, which can effectively reduce the accessibility and affinity of organic molecules to the inner pore where the majority of the carbon surface

area is located. Consequently the overall adsorption capacity is reduced. Water cluster formation is especially important in the adsorption of SOCs at dilute concentrations typically encountered in environmental treatment systems.

### 2.3 Adsorption of DOM onto activated carbons and activated carbon fibers

Adsorption of DOM onto GACs and ACFs has been widely investigated. Some investigation results closely relevant to this study are discussed in this section.

The adsorption of DOM separated from the influent of a treatment plant in Charleston, South Carolina by two ACFs (ACF10 and ACF20H) and one GAC (HD3000) was investigated by Dastgheib et. al (2004). ACF10 had about 90% of its pore volume in pores less than 10 Å, ACF20 had 98% of its total volume in pores <20 Å and about 67% volume in pores <10 Å in size. However, ACF10 and ACF20 had similar volumes in <10 Å pore size range. HD3000 was predominantly mesoporous and was the only adsorbent in this study having pores >30 Å in size. The results showed that ACF10 displayed negligible DOM uptake implying that pores <10 Å in size are nearly inaccessible to the DOM molecules. However, ACF20H did show some amount of DOM uptake. Therefore, it was concluded that some components of DOM access and adsorb in the 10-20 Å pore size region but not pores <10 Å. The most mesoporous HD3000 showed the highest DOM uptake among the three adsorbents. The size exclusion chromatography (SEC) results showed that only low molecular weight DOM components were removed by ACF20 indicating that only the low molecular weight fractions of DOM are accessible to pores <20 Å in size (Cheng et al., 2005).

In another study, adsorption of humic acids and a river water DOM onto a microporous GAC (F400) was investigated (Kilduff et al., 1996). It was found that the microporous adsorbent preferentially removed the low molecular weight humic acid components. Several studies also investigated the role of carbon pore size distribution in DOM adsorption, and it was found that DOM adsorption increased with an increase in secondary micropore and mesopore volumes (Bjelopavlic et al., 1999 and Newcombe, G., 1999).

#### 2.4 Effect of dissolved organic matter (DOM) on the adsorption of SOC by activated carbons

All sources of drinking water contain natural organic matter (NOM). NOM presents in either dissolved or colloidal, or particulate forms. NOM in water comes from internal and/or external sources. Internal sources include organic matter derived from the algae, bacteria, and other biota growing in water body, while external sources include organic matter that makes its way to the source water via run-off from surrounding terrestrial water sheds and/or from infiltration from the groundwater (Thurman, 1985; Croue et al., 2003). With respect to the application of activated carbon adsorption in water treatment, the most problematic components of NOM is the dissolved organic matter (DOM) fraction, a heterogeneous mix of hydrophilic acids, proteins, lipids, carboxylic acids, polysaccharides, amino acids, and hydrocarbons. DOM is operationally defined as constituents of NOM passing through a 0.45  $\mu\text{m}$  filter. Due to its heterogeneous nature, DOM concentrations in fresh waters are often quantified with surrogate parameters like total organic carbon (TOC) and/or dissolved organic carbon

(DOC). In a recent nationwide survey, the lowest and highest DOC concentrations reported in the United States were  $< 0.35$  and  $27.5$  mg/L, respectively, with the mean concentration in the water sources being around  $2.8$  mg/L (McGuire et al., 2002). The DOM concentration in fresh waters is usually orders of magnitude higher than that of target SOC. In addition, the physicochemical characteristics of DOM are site specific and vary greatly from one source water to another.

The effect of DOM on the adsorption of SOCs by activated carbons has been investigated in numerous studies. The adsorption capacities of activated carbons to trace compounds, typically present at concentrations of microgram or nanogram per liter level were reduced under both simultaneous and preloading (approach wherein the carbon is first equilibrated with the DOM and then the target SOC is introduced in the system) adsorption conditions (Kilduff and Karanfil, 2002; Carter et al., 1992; Najm et al., 1990; Summers et al., 1989). In a study investigating the removal of trichloroethylene (TCE) from a water source containing natural organics, it was found that in a GAC adsorption column, the best way to describe the reduction in TCE adsorption capacity due to the presence of DOM was by the preloading isotherm approach (Karanfil, 2006). This is due to the polydisperse physical and chemical properties of DOM which lead to the formation of extended adsorption zones in the fixed-bed activated carbon adsorbers. As a result the mass transfer zone of the DOM components moves ahead of that of the target SOC compound. Due to the faster movement of the mass transfer zone of DOM compared to that of SOC, the fresh GAC in the lower layers of the adsorber is continuously preloaded or fouled by the DOM components prior to SOC adsorption. This preloaded GAC

therefore has reduced adsorption capacity for subsequent target SOC compound (Karanfil, 2006)

It has been proposed that direct competition for adsorption sites and pore blockage are the two primary competition mechanisms by which DOM interferes the adsorption of trace organic compounds (Carter et al., 1992). Small, strongly adsorbing DOM molecules, comparable in size to target SOC compound directly compete for adsorption sites and causing a reduction in the adsorption capacity of the target SOC. In contrast, large DOM molecules that may not adsorb on the same sites as the target compound are capable of blocking the pore entrances through which the target compound has to travel to access its final adsorption sites (Carter et al., 1992).

In an earlier study investigating the removal of five taste and odor organic compounds of nanogram per liter levels in water supplies, it was observed that presence of background organics reduced the adsorption capacity of activated carbon to odor-causing compounds geosmin and 2-methylisoborneol (MIB) (Lalezary et al., 1986). Competition between MIB and DOM was also investigated by Newcombe and co-researchers using a series of PAC with different pore size distribution (Newcombe et al., 2002). They compared the adsorption of MIB after 4 hours of contact time and also under equilibrium conditions (3-6 days of contact time) using DOM obtained from a reservoir. They found that microporous carbons showed higher equilibrium capacities but slower kinetics for the adsorption of MIB. The low molecular weight NOM compounds were found to be the most competitive. Some evidence of pore blockage and/or restriction was also observed. The microporous carbons were significantly affected by the low molecular

weight fraction of NOM, while the mesoporous carbons were impacted by the high molecular weight NOM compounds. The order of MIB removal capacity of the carbons obtained in the presence of smallest size DOM with contact time less than 1 hour was different from that measured at equilibrium conditions. Therefore, they concluded that the performance of PAC depends on the contact time.

Matsui et al. (2002) investigated the removal of two pesticides of similar molecular size: simazine and asulam, from NOM-containing water using pilot-scale GAC adsorbers over a period of three years. They found that the SOC removal percentage obtained at any preloading time and bed depth was independent of the liquid-phase SOC concentration. Asulam due to its highly polar nature was less capable of displacing preadsorbed NOM than simazine. This meant that the fraction of preloaded NOM affecting the adsorption of asulam differed from the fraction affecting the adsorption of simazine. They also found that the mass transfer zone of the NOM fraction competing with asulam traveled more rapidly through the adsorber as compared to the mass transfer zone of the NOM fraction that competed with simazine. As mentioned earlier, this effect was attributed to the difference in the adsorption affinity of the two SOCs the weakly adsorbing asulam was less capable of displacing the preloaded NOM.

Several studies have been performed to investigate the role of carbon surface chemistry and pore size distribution on the competitive adsorption of SOC and NOM. The effects of physical and chemical properties of activated carbon on the simultaneous adsorption of SOC and NOM were investigated by Quinlivan et al. (2005). The SOCs used in this study were a relatively hydrophilic fuel additive, methyl tertiary-butyl ether,

(MTBE) and relatively hydrophobic solvent, TCE. The adsorbent matrix consists of twelve ACFs with three activation levels and four surface chemistry properties and three commercially available GACs. The results indicated that both in the presence of NOM, the percent reductions in the TCE and MTBE adsorption capacities compared to that of single-solute adsorption were not significantly affected by the chemical characteristics of the activated carbon. The hydrophobic carbons were found to be more effective than the hydrophilic ones for both TCE and MTBE adsorption because of the interference of the water clusters on the adsorption of hydrophilic carbons. They also claimed that, with respect to pore structure, the adsorbents should possess a large volume of micropores with widths about 1.5 times of the kinetic diameter of the target adsorbate. They also stated that an adsorbent, to be effective and to prevent pore blockage resulted from NOM adsorption, should possess a pore size distribution extending to the widths that are approximately twice of the kinetic diameter of the target adsorbate.

Karanfil and Kilduff (1999) showed that for single solute TCE and trichlorobenzene adsorption onto activated carbons, surface acidity played an important role: increasing surface acidity or polarity of the carbon reduced the adsorption of hydrophobic SOC. Heat treatment in an inert atmosphere was used to decrease surface acidity and polarity in this study, which increased the adsorption of SOC (Karanfil and Kilduff., 1999). Kilduff et al. (2002) evaluated the effects of adsorbent surface chemistry on TCE adsorption capacities of NOM preloaded activated carbons. The percent decrease in TCE adsorption capacity resulting from NOM preloading became lower with increasing surface acidity for coal-based activated carbons. However, the single-solute

TCE adsorption capacity also decreased with decreasing surface acidity, and the latter effect dominated. Therefore, the most hydrophobic adsorbent, i.e. the activated carbon with the lowest surface acidity, exhibited the largest TCE adsorption capacity following NOM preloading. For wood based activated carbons, however, decreasing the surface acidity did not increase the effect of NOM preloading on the percent reduction in TCE adsorption capacity. The adsorbent with the lowest surface acidity among the wood-based activated carbons was again the most effective for TCE adsorption with/without the presence of NOM (Kilduff et al., 2002).

Pelekani and Snoeyink (1999) examined the effect of DOM on the adsorption of atrazine by two activated carbons fibers: ACF10 (a microporous activated carbon fiber) and ACF25 (a mesoporous activated carbon fiber). It was found that the adsorption of ACF10 to atrazine was significantly reduced even its DOM uptake is slight. By contrast, the adsorption capacity of atrazine of ACF25 showing relatively high DOM uptake, even though was reduced but not to the same extent as in the case of ACF10. The researchers concluded that the DOM competitive effect for ACF10 was due to pore blockage and that for ACF25 was due to direct site competition. They therefore proposed that high secondary micropore volume can reduce the impact of DOM on SOC adsorption. The researchers further strengthened their claim by performing more experiments using atrazine and dyes of molecular sizes comparable to that of atrazine. For dyes with similar molecular size as that of atrazine (in the 10-20 Å size range), wide pore size distribution and high volume in the secondary micropore region significantly reduced the competition between the two adsorbates. A similar investigation (Ebie et al, 2000) showed that the

DOM-SOC competition can be reduced by broadening the pore size distribution and increasing pore volume above 3 nm.

Adsorption of TCE in the presence of different background DOMs and their hydrophobic and transphilic fractions onto several carbonaceous sorbents including ACF10 was performed by Karanfil et al. (2006). In this study, the carbons were first contacted with DOM for two weeks (preloaded) and subsequently TCE was spiked into the reactors and allowed to reach equilibrium. The activated carbons with significant DOM uptake showed significantly reduced TCE adsorption. However, for adsorbents demonstrating very little DOM uptake, such as ACF10 shown in previous studies, the impact of DOM preloading on the TCE adsorption was unapparent. This suggested the potential of using microporous carbons as molecular sieve, whereby the bulky DOM molecules are 'sieved out' and only the small SOC molecules are removed from the solution by adsorption in the pores inaccessible to the DOM molecules.

The role of solution chemistry on the NOM preloading of GAC and subsequent TCE adsorption was investigated by Kilduff and Karanfil (2002). They found that an increase in solution ionic strength, calcium concentration (within solubility limits) and dissolved oxygen enhanced the DOM adsorption. Consequently, greater reductions in TCE adsorption occurred for a given percentage of TOC removal. They also found that the reduction in TCE uptake was only dependent on the DOM adsorbed during preloading not the ionic strength or calcium concentration. Therefore they concluded that the DOM competition could be significant at high DOM preloading condition as a result

of high ionic strength, low pH, high dissolved oxygen, or significant divalent calcium concentrations.

In summary, the activated carbon adsorption efficiency to SOC<sub>s</sub> was reduced by DOM competition due to: (i) the concentration of DOM (mg/L) is orders of magnitude higher than that of the target SOC compound ( $\mu\text{g/L}$  or even  $\text{ng/L}$ ); (ii) DOM hinders SOC adsorption onto activated carbon by pore blockage and it also directly competes with the target SOC for adsorption sites on the activated carbon surface; (iii) DOM, a big and bulky molecule has the ability to bind at multiple sites and does not desorb easily from the carbon surface. The extent of site competition and pore blockage effects of DOM on the SOC adsorption depends on: (i) the concentrations of both DOM and the target SOC, (ii) the physicochemical properties of the DOM mixture, (iii) the molecular structure and dimensions of the SOC, (iv) pore size distribution and surface chemistry of the activated carbon, (v) the chemistry of the source water, and (vi) contact time (Karanfil, 2006).

In practical applications, the competitive adsorption of DOM and the target SOC compound is unavoidable. This often results in the operation life of the GAC adsorbers being drastically reduced and an increase in the carbon usage rate. Overall, the presence of DOM impairs the performance of both fixed-bed carbon adsorber and PAC applications.



## CHAPTER 3

### RESEARCH OBJECTIVES

The main objective of this study was to conduct a systematic experimental investigation to test these proposed series of hypotheses and determine approaches to mitigate DOM competition on the SOC adsorption.

Considering the literature review presented in the previous chapter and the fact that the approximate diameters of aquatic DOM in the range of 10 to 17 Å reported in several studies (Moore et al., 2001), it has been hypothesized in this work that 10 Å represents an important cutoff value for developing strategies to minimize the impact of DOM on SOC adsorption (Karanfil, et al., 2006). It was postulated that for the adsorption of SOC with target adsorption region in pores less than <10 Å (e.g., TCE), one possibility to mitigate the DOM competition is to use a very microporous activated carbons having mainly pores <10 Å, which are accessible to the SOC but not the DOM components. In this case, the activated carbon is expected to act as a molecular sieve, minimizing the competition from the DOM molecules, as long as they do not completely block the carbon pores. The second possibility is to use an activated carbon with a broad pore size distribution including appreciable pore volumes in both transitional pores (i.e., secondary micropores (10-20 Å), mesopores (20-50 Å)) to accommodate DOM molecules and primary micropores (i.e., <10 Å) for the target SOC (e.g., TCE).

It is further postulated that if the optimum region for the SOC adsorption is in pores >10 Å (e.g., atrazine), where the optimum pore region of target SOC and some

DOM components overlaps, then activated carbons with high pore volumes in the secondary micropores and mesopores should be selected to reduce the DOM competition.

Two SOC adsorbing in the significantly different pore size regions, TCE and atrazine, were selected as the target compounds to experimentally test these hypotheses. As discussed earlier, several studies have investigated the adsorption of these two compounds individually (Karanfil and Dastgheib, 2004; Karanfil et al., 2006; Pelekani and Snoeyink, 1999, 2000, 2001), however their adsorption on a set of adsorbents with different pore size distributions in the presence of the same background DOM has not been compared side by side. Since the hypotheses postulated above are mainly derived from many observations obtained using carbon fibers (Pelekani and Snoeyink, 2000; Karanfil and Dastgheib, 2004), and it is known that activated carbon fibers and activated carbons have important differences in their pore structures (Figure 2.1), the selected adsorbents for this study consisted of five activated carbons (four GACs and one ACF) to examine the proposed hypotheses from a practical application perspective. The ACF was selected for the purpose of comparing the results between GACs and ACFs.

The selected adsorbents covered a wide and gradually increasing pore size distribution, ranging from very microporous to carbons with some degree of mesoporosity and finally to a predominantly mesoporous adsorbent. These adsorbents were selected because they also had relatively similar surface acidity and hydrophobicity. Similar surface chemistry was an important consideration in the adsorbent selection because the main goal of the study was to obtain a better understanding on the interplay between the optimum adsorption pore size regions of the target SOC and the DOM

controlling the SOC-DOM competitive adsorption. A secondary objective in the study was to conduct a limited number of kinetic experiments to gain additional understanding of the DOC-SOC competitive adsorption.



## CHAPTER 4

### MATERIALS AND METHODS

#### 4.1 Adsorbents

Four granular activated carbons (two coconut shell-based: OLC (Calgon Carbon Corporation) and CR3140C (Carbon Resources); two coal-based: F400 (Calgon Carbon Corporation) and HD4000 (Norit Inc.)) and a phenol formaldehyde based activated carbon fiber ACF10 (American Kynol Inc.) were used in this project.

Virgin GAC samples were crushed, sieved and washed with DDW (distilled and deionized water, then dried at 90°C and stored in sealed containers for later experimental use. The GAC particles collected between US standard sieves of #80 and #100 mesh size (150  $\mu\text{m}$  < diameter < 180  $\mu\text{m}$ ) were used in the experiments. ACF was cut into very small pieces and was used in the form of small fiber threads.

##### 4.1.1 Treatment of the selected adsorbents

Virgin OLC, CR3140C (from here on referred to as CRC) and ACF10 were used without any further treatment in this study.

Approximately 5-10 g of F400 was heat treated under helium (He) flow for 2 hours at 900°C in a quartz reactor within a tubular furnace. The primary aim of this heat treatment was to remove most of oxygen surface functionalities (Puri, 1970), thus decrease the surface acidity of the carbon (Karanfil and Dastgheib, 2004). It has been

shown that the presence of oxygen-containing surface functionalities has negative impact on adsorption of SOCs due to the formation of water clusters around the heteroatoms on the surface of the activated carbon (Karanfil et al., 2006). This sample was labeled as F400He, where He stands for the helium treatment.

Steam treatment was applied on HD4000 carbon in order to enlarge the pores and obtain a significantly mesoporous carbon. Steam treatment, to some extent, also decreased the surface acidity of the carbon. About 150 g carbon sample was placed into a combustion quartz tube within a furnace. The temperature was raised to 800°C at 30°C/min under nitrogen flow at a rate of ~100 cm<sup>3</sup>/min. Then, the gas flow was switched to high temperature steam at ~30 g H<sub>2</sub>O/min for 2, 3 or 4 hrs, respectively. After the steam treatment, the furnace was shutdown and the gas flow was switched back to nitrogen until the furnace was cooled down to room temperature. The treated carbon sample was then washed repeatedly with DDW and dried at 90°C. These modifications were performed by Dr. Wei Cheng, who at the time was a doctoral student in Dr. Karanfil's research group.

## 4.2 Adsorbates

Trichloroethylene (TCE) and atrazine are the two adsorbates selected for this study. TCE is a planar molecule with dimensions of 6.6 × 6.2 × 3.6 Å (Fig 4.1), and atrazine molecule is a relatively bulky with dimensions of 11.5 × 10.9 × 6.7 Å (Fig 4.2).

TCE (Mallinckrodt Baker Inc.) stock solution was prepared in methanol and stored in a sealed bottle under refrigeration. TCE was analyzed after hexane extraction on

a Hewlett Packard 5890 gas chromatograph equipped with an electron-capture detector. A mixture of  $^{14}\text{C}$  radio-labeled atrazine (American Radiolabeled Chemicals, Inc.) and non-labeled atrazine (Sigma-Aldrich) was used in the experiments. Both atrazine stock solutions were prepared in acetone and stored in separate sealed bottles under refrigeration. Only the content of  $^{14}\text{C}$  atrazine was analyzed in the aqueous phase experiments assuming that the percent reduction observed in  $^{14}\text{C}$  atrazine is the same as that of the total atrazine content. The atrazine concentration was determined by analyzing the  $^{14}\text{C}$  atrazine in a mixture of 1mL solution and 10 mL liquid scintillation cocktail (Ultima Gold, Perkin Elmer) with a Wallac 1415 Liquid Scintillation Counter (LSC).

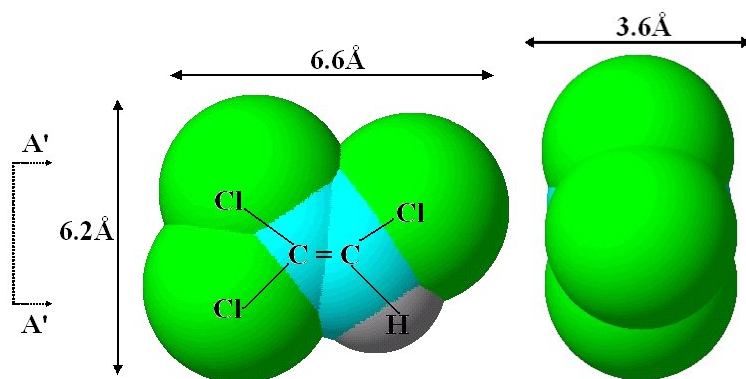


Figure 4.1 Trichloroethylene molecule

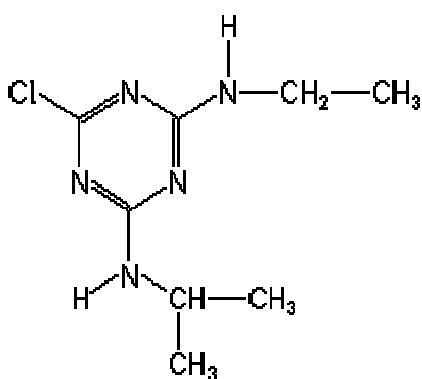
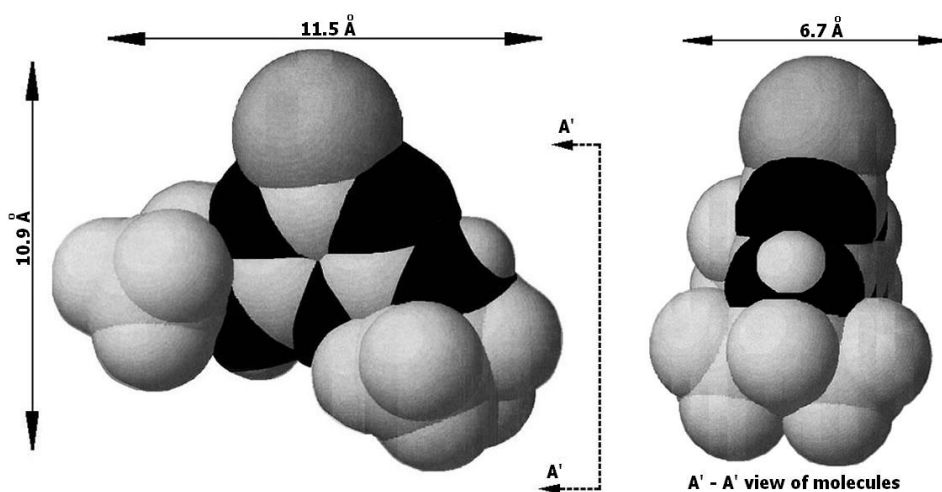


Figure 4.2 Atrazine molecule

### 4.3 DOM solution

DOM was collected from the influent of Spartanburg drinking water treatment plant in South Carolina (USA) using a reverse osmosis (RO) system, as described elsewhere (Kitis et al., 2001). Mass balance calculations showed that the DOM recoveries during RO isolation were over 87%, indicating that the majority of the DOM in the source was captured. The DOM had a specific ultraviolet absorbance (SUVA<sub>254</sub>) of 3.2 L/mg-m. The RO concentrate was diluted to the desired dissolved organic carbon (DOC) concentration before the SOC competition adsorption experiments. The DOM collection,

RO isolation and mass balance calculations were performed by Ms. Olivia Orr, who is student in Dr. Karanfil's research group and Dr. Hoechoel Song, who is a post doctoral research associate in Dr. Karanfil's research group.

#### 4.4 Characterization of the adsorbents

The characteristics of adsorbents were determined from nitrogen adsorption results: (i) BET equation for surface area, (ii) nitrogen uptake at relative pressure around 0.98 for total pore volume, and (iii) Micromeritics' density functional theory (DFT) for pore size distribution. The pH of the point of zero charge ( $\text{pH}_{\text{pzc}}$ ) values were measured to characterize the carbon surface acidity. Water vapor isotherms of the adsorbents were volumetrically obtained from the low relative pressures of  $10^{-2}$  up to relative pressures close to one at 273.15 K using the Micromeritics ASAP 2010 surface analyzer. Carbon characterization was performed by Dr. Yangping Guo, who is a post doctoral research associate in Dr. Karanfil's laboratory.

##### 4.4.1 Surface area and pore size distribution

Nitrogen gas adsorption isotherms, volumetrically obtained in the relative pressure range of  $10^{-6}$  to 1 at 77 K on a Micromeritics ASAP 2010 Physisorption Analyzer, was used to determine the surface area and pore size distribution of the samples. Surface area was calculated from Brunauer-Emmett-Teller (BET) equation. The relative pressure range used for the BET calculation was 0.01 to 0.1. Micromeritics DFT software coming with the analyzer was used to determine the pore size distribution of the

activated carbon samples. A graphite model with slit shape pore geometry was assumed in the pore size distribution calculation. The adsorbed volume of the nitrogen near saturation point ( $P/P_0 = 0.98$ ) was used to determine the total pore volume. Triplicate results of randomly selected samples were used to determine the reproducibility of the data and the RSD (relative standard deviation) of the BET surface area, micro pore volume and the total pore volume was lower than 10%.

#### 4.4.1.1 Brunauer-Emmett-Teller (BET) model

Brunauer et al. (1938) generalized a form of Langmuir isotherm by incorporating the concept of multilayer adsorption to formulate the BET model, which is used to determine the surface area of a sample based on the assumption that the forces responsible for the binding energy in multimolecular layer adsorption are the same as those involved in the condensation of gases. The BET equation was obtained by equating the rate of condensation of the molecules onto an already adsorbed layer to the rate of evaporation from that layer and summing for an infinite number of layers. Rearranging that equation in a linear form results in following BET equation (Webb and Orr, 1997):

$$\frac{P}{V_a (P_0 - P)} = \frac{1}{V_m C} + \frac{C - 1}{V_m C} \left( \frac{P}{P_0} \right)$$

Where

$P_0$ = saturation pressure of the adsorption gas

$V_a$ = quantity of gas adsorbed at pressure P

$V_m$  = quantity of gas adsorbed when the entire surface is covered with a monomolecular layer

$C$  = constant.

The volume of the monolayer ( $V_m$ ) can be obtained by plotting  $P / (V_a (P_0 - P))$  Vs  $P/P_0$ , where  $1/V_m C$  is the intercept and  $(C-1) / V_m C$  is the slope of the linear plot. It is possible to determine the surface area of the sample by knowing the volume of the monolayer adsorption and the area occupied by a single adsorbate molecule:  $16.2 \text{ \AA}^2$  for nitrogen,  $21.0 \text{ \AA}^2$  for krypton,  $14.2 \text{ \AA}^2$  for argon and  $17.0 \text{ \AA}^2$  for  $\text{CO}_2$  (Webb and Orr, 1997).

#### 4.4.2 pH of the point of zero charge ( $\text{pH}_{\text{pzc}}$ )

The  $\text{pH}_{\text{pzc}}$  was determined according to the method described in Karanfil and Dastgheib (2004). Distilled and deionized water (DDW) was initially boiled to remove dissolved  $\text{CO}_2$ . The boiled DDW was used to prepare 0.1M NaCl solutions with the pH in the range of pH 2 to pH 11 adjusted with either 0.5N HCl or 0.5N NaOH solutions. In 25 ml vials, 100 mg of activated carbon sample was mixed with 20 ml of the 0.1M NaCl solutions of different pH values. The vials were shaken at 200 rpm on a table shaker at room temperature for 48 hours, and then were left on a bench to allow the activated carbons to settle down. The final pH of the solution was measured using a pH meter. The  $\text{pH}_{\text{pzc}}$  was determined as the pH of the NaCl solution which did not change its pH after contacting with the carbon samples. Duplicate runs were also performed for randomly selected samples and the reproducibility of the measurements was within  $\pm 0.2$  units.

#### 4.4.3 Water vapor adsorption

Water vapor adsorption isotherms were volumetrically obtained at 273.15K using the Micromeritics ASAP 2010 Physisorption Analyzer for all the adsorbents to assess their surface hydrophilicity (Karanfil and Dastgheib, 2004). The water vapor uptakes in the low relative pressure ( $P/P_0$ ) range of 0.0 to 0.4 have been related to the extent of water cluster formation around the hydrophilic sites (Karanfil et al., 2006; Moula and Kaneko, 2003). Approximately 50-100 mg of carbon sample was degassed for a period of 1 hour at 90°C and overnight at 200°C to remove the moisture and other adsorbed vapors/gases. The degassed samples were then transferred to the analysis port and adsorption data points were collected. Data were collected in the relative pressure range of  $10^{-4}$  - 1. The water vapor adsorption experiments were performed by Dr. Yangping Guo.

#### 4.5 Isotherm experiments

Single Solute Isotherms: Constant dose bottle point technique was used for the single solute isotherm experiments. Five mg of carbon was equilibrated with 133 mL SOC solution of different concentrations in amber glass bottles (headspace free) on a rotary tumbler for two weeks at room temperature ( $21 \pm 3^\circ\text{C}$ ). After equilibration period, final SOC concentration was analyzed.

Preloading Isotherms: Five mg of carbon was first contacted with 133 mL DOM solution (at two different concentrations, 5 and 20 mg DOC/L) in a series of amber glass bottles for two weeks. Then predetermined amounts of SOC stock solution (at  $\mu\text{L}$  levels) was directly spiked into the bottles and allowed to equilibrate for another two weeks. All

isotherm experiments, single solute and preloading, were performed in a carbonate buffer of pH 7 and at room temperature ( $21\pm 3^\circ\text{C}$ ).

DOM adsorption Isotherms: Constant-dose bottle point isotherm experiments with a wide range of initial DOM concentrations were performed for the MB water. Fifty milligrams of carbon was placed in each ~130 mL amber bottle. One hundred milliliters of DOM solution, having a target concentration between 0 and 20 mg/L TOC, prepared in a 0.01 M NaCl background (providing approximately 2000  $\mu\text{S}/\text{min}$  conductivity for all of the solutions), were added in each bottle. Two types of blanks served as controls during the isotherm experiments: bottles containing solutions with various DOM concentrations but without any adsorbent, and bottles containing carbons in contact with distilled and deionized water. Sealed bottles were placed on a rotary tumbler for 14 days at room temperature ( $22\pm 2^\circ\text{C}$ ). The pH of the water during the adsorption experiments ranged from 6.5 to 7.5. After two weeks of contact time, solutions (including blanks) were filtered using a pre-washed membrane filter (0.45 $\mu\text{m}$  Supor, Gelman, Ann Arbor, Michigan, USA), and analyzed for  $\text{UV}_{254}$  absorbance using a spectrophotometer (DU-640, Beckman, Fullerton, California, USA), and dissolved organic carbon (DOC) concentration using a high temperature combustion analyzer (TOC-5000, Shimadzu, Kyoto, Japan). The DOM adsorption isotherms were performed by Dr. Wei Cheng.

#### 4.6 Kinetics experiments

Single Solute Kinetics: In distilled and deionized water, 5 mg of adsorbent was contacted with 133 mL of SOC solution of the same concentration in a series of amber glass bottles (headspace free) on a rotary tumbler at room temperature ( $21\pm 3^{\circ}\text{C}$ ). Samples were removed at periodic intervals for analysis in order to obtain the adsorption kinetics. A different bottle reactor was used for each point in order to maintain constant dose for all the sample points.

Kinetics in the Presence of 5 mg/L Background DOM: The experimental setup for these experiments was similar to the DDW kinetic experiments, except that a background DOM solution of 5 mg DOC/L was used instead of DDW.

## CHAPTER 5

### RESULTS AND DISCUSSION

#### 5.1 Characterization of the adsorbents

Surface area and pore size distribution,  $\text{pH}_{\text{pzc}}$ , and water adsorption characterization results were obtained for all the five activated carbons (Table 5.1). The pore size distributions for all five adsorbents are presented graphically in Figure 5.1. This section will present a discussion of the characterization results. The results indicated that the carbons ranged from extremely microporous, to some degree of mesoporous and primarily mesoporous. The ratio of available pore volume in the primary micropores ( $<10 \text{ \AA}$ ) to the pore volume available in pores less than  $1000 \text{ \AA}$  in size indicated that there were three microporous carbons. ACF10 was the most microporous adsorbent, with 90% of its volume in pores less than  $1000 \text{ \AA}$  being present in pores  $<10 \text{ \AA}$  in size. OLC and CRC, the two coconut-shell based activated carbons showed relatively similar pore size distributions and were predominantly microporous. F400He had lower pore volume available in pores  $<10 \text{ \AA}$  as compared to ACF10, OLC, and CRC but was higher than HD4000ST. Finally, HD4000ST had the least primary micropore volume and the highest mesopore volume ( $>20 \text{ \AA}$ ) among all five studied adsorbents. HD4000ST however, had comparable secondary micropore ( $10\text{-}20 \text{ \AA}$ ) volume to CRC and F400He.

F400He had the highest pore volume in the secondary micropores ( $10\text{-}20 \text{ \AA}$ ). CRC and HD4000ST showed similar pore volumes but were slightly lower than F400He. OLC had significantly lower volume in the pore size range of  $10\text{-}20 \text{ \AA}$  than the three

carbons mentioned above (about 50% lower than that of F400He). ACF10 had the lowest volume in this pore size range, which is about 85% lower than that of F400He. In pores  $> 20 \text{ \AA}$ , ACF10, OLC and CRC had negligible pore volumes. F400He showed some pore volume in this size range while HD4000ST had the highest pore volume available in this pore size range. Overall, these results indicated that the adsorbent matrix consisted of carbons with a gradually broadening pore size distribution, which in terms of being microporous to mesoporous followed the order of  $\text{ACF10} > \text{OLC} \geq \text{CRC} > \text{F400He} > \text{HD4000ST}$ .

The  $\text{pH}_{\text{pzc}}$  values of the five carbons ranged from 8.6 to 10.9, indicating that all carbons used in this study are basic in nature. The high  $\text{pH}_{\text{pzc}}$  values also signify the absence of various acidic groups on the surface of the activated carbon, thus all the carbons are relatively hydrophobic in nature (Karanfil and Dastgheib, 2004). However, the direct information about the surface hydrophilicity was obtained by performing water vapor adsorption experiments. The results of the water vapor adsorption are displayed in Figure 5.2. The water vapor uptake at low relative pressure ( $P/P_0$ ) range (e.g., 0.0 to 0.4) has been related to the extent of water cluster formation or the degree of hydrophilicity (or polarity) of the carbon surface (Karanfil et. al, 2004; Mowla and Kaneko, 2003). In this study, the water vapor uptake at a relative pressure of 0.4 was selected to represent the hydrophilicity of the five activated carbons. The order of water vapor uptake was  $\text{HD4000ST} \approx \text{F400He} < \text{OLC} \approx \text{CRC} < \text{ACF10}$ . However, these values, when compared to those measured in the previous work for a series of virgin and surface modified

activated carbons (Karanfil and Dastgheib, 2004), indicated that these adsorbents had relatively hydrophobic surfaces.

Table 5.1 Physicochemical characteristics of the carbons

| Adsorbent | Pore Vol. Distribution |                    |                    |                    |                    |                    |                    |               | pH <sub>pzc</sub> | Water Uptake<br>at P/P <sub>o</sub> =0.4 |
|-----------|------------------------|--------------------|--------------------|--------------------|--------------------|--------------------|--------------------|---------------|-------------------|--|
|           | S <sub>BET</sub>       | V <sub>t</sub>     | 5-8 Å              | <10 Å              | 10-20<br>Å         | >20 Å              | <1000 Å            | <10 Å/<1000 Å |                   |  |
|           | m <sup>2</sup> /g      | cm <sup>3</sup> /g | cm <sup>3</sup> /g | cm <sup>3</sup> /g | cm <sup>3</sup> /g | cm <sup>3</sup> /g | cm <sup>3</sup> /g | %             |                   |  |
| ACF10     | 941                    | 0.54               | 0.24               | 0.26               | 0.03               | 0.00               | 0.29               | 90            | 8.6               | 0.108                                    |
| OLC       | 987                    | 0.42               | 0.19               | 0.25               | 0.07               | 0.02               | 0.35               | 71            | 8.9               | 0.060                                    |
| CRC       | 1120                   | 0.46               | 0.21               | 0.27               | 0.11               | 0.02               | 0.39               | 69            | 10.9              | 0.061                                    |
| F400He    | 1037                   | 0.51               | 0.17               | 0.21               | 0.13               | 0.10               | 0.43               | 49            | 9.8               | 0.033                                    |
| HD4000ST  | 932                    | 0.96               | 0.13               | 0.14               | 0.11               | 0.49               | 0.74               | 29            | 8.7               | 0.035                                    |

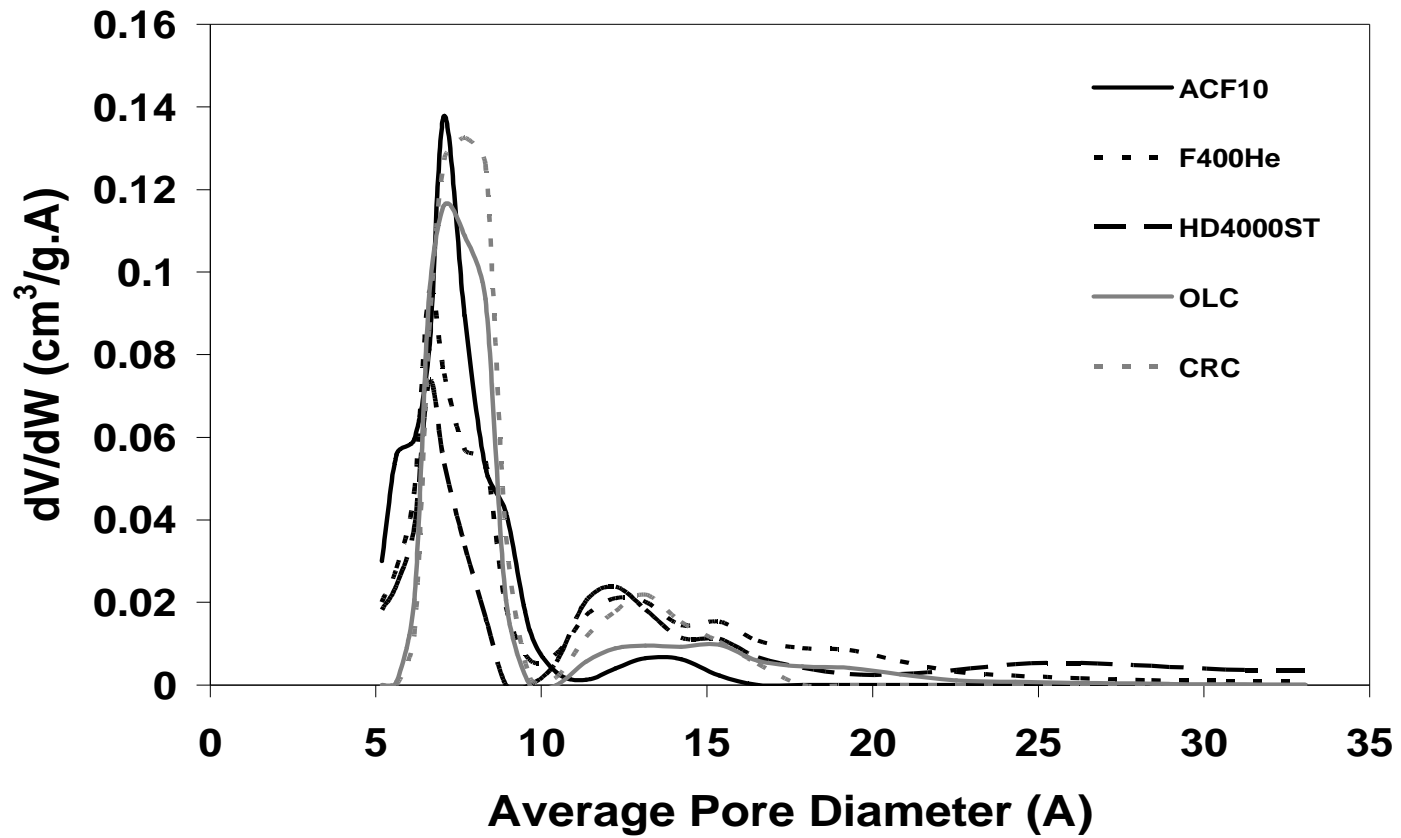


Figure 5.1 Pore size distribution of all five carbons

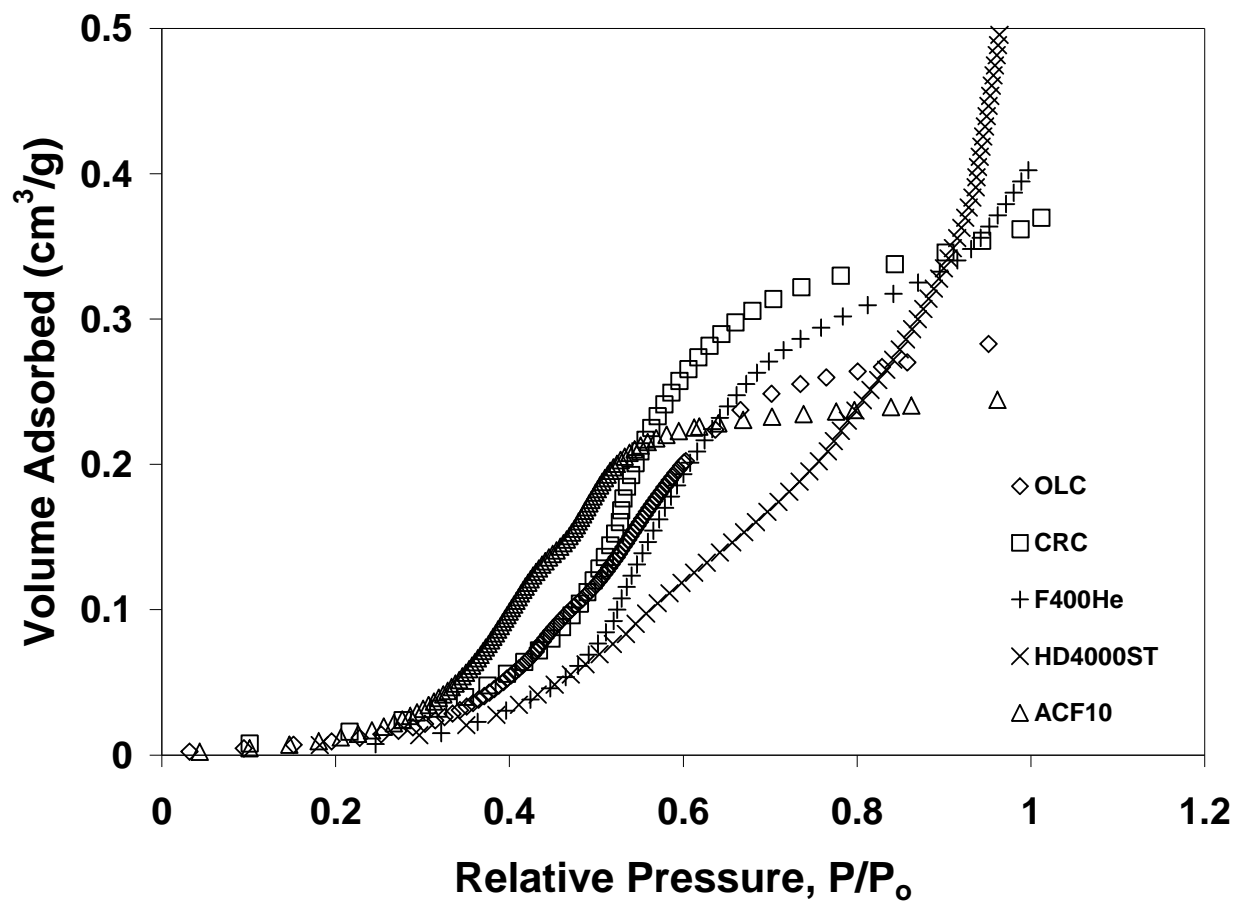


Figure 5.2 Water vapor adsorption for all activated carbons

## 5.2 TCE isotherms

The single solute TCE adsorption isotherms for all five activated carbons are shown in Figure 5.3. At low equilibrium liquid phase concentrations (1-10  $\mu\text{g/L}$ ), the TCE uptake was comparable for all carbons, however, at high concentrations the carbons with more volume in pores  $<10 \text{ \AA}$  showed higher uptakes. Similar TCE uptakes by all carbons corresponding at low equilibrium liquid phase concentrations is due to the fact that all carbons have orders of magnitudes higher primary micropore volumes than the required volume for TCE adsorption at this condition (Karanfil and Dastgheib, 2004). The effect of adsorbent on the TCE uptake emerged with increasing equilibrium concentration. At equilibrium concentration of 1000  $\mu\text{g TCE/L}$ , ACF10 and OLC show the highest uptakes followed by CRC and F400He, which show similar uptake. Finally, HD4000ST showed the lowest TCE uptake among all the carbons investigated in this study.

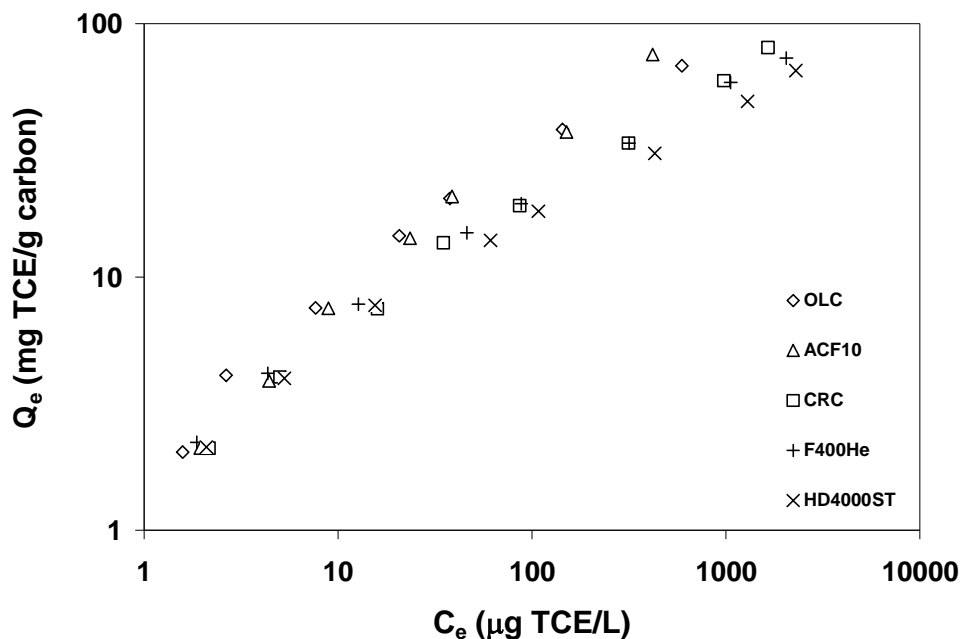


Figure 5.3 Single solute TCE adsorption in DDW

The density of TCE at 25°C is 1.46 g/mL (CRC Handbook of Chemistry and Physics, 1992), therefore the adsorbed TCE molecules occupy approximately 0.07 cm<sup>3</sup>/g pore volume at the highest surface loadings, ~ 100 mg TCE/g carbon, of the isotherms. Also, the primary micropore (<10 Å) volumes (i.e., the important pore size region for TCE adsorption) of all adsorbents were two to four times higher than the pore volume required to accommodate the adsorbed TCE molecules. In Figure 5.3, the order of uptakes by different carbons at high TCE concentrations increased with increasing primary micropore volumes of the carbons. The only exception was CRC, which had the highest primary micropore volume but showed lower TCE uptake than OLC and ACF10. In a previous study, it was concluded that 5-8 Å is the optimum TCE adsorption region

within the pores  $<10 \text{ \AA}$  (Karanfil and Dastgheib, 2004). AFC10 had the highest pore volume in this pore region and highest TCE uptake. Although CRC had slightly higher pore volumes in this pore size region than OLC, it showed lower TCE uptake than OLC.

These results showed that (i) the sorbents having higher amount of pores with sizes approaching the dimensions of the adsorbate molecules show higher uptakes, probably due to higher adsorption energies resulting from multiple contact points between the adsorbate molecules and the adsorbent, (ii) it appears that there are some pore structure effects that are not completely captured by pore size distribution analysis. For example, OLC showed higher TCE uptake than CRC at high equilibrium concentrations despite the latter having higher pore volumes in  $<10 \text{ \AA}$  and  $5\text{-}8 \text{ \AA}$  pore size regions than the former. Furthermore, OLC and F400 showed similar uptakes at high equilibrium concentrations, although the former had higher pore volumes in  $<10 \text{ \AA}$  and  $5\text{-}8 \text{ \AA}$  pore size regions than the latter. In all these cases, the volumes in the mentioned pore size regions were not limiting factors; they were at least twice the amount required by the adsorbed TCE molecules, and (iii) the BET surface area and total pore volume are not the factors controlling the adsorption.

Preloading experiments were performed at two DOM concentrations, 5 and 20 mg DOC/L (Figure 5.4 and 5.5). The single solute DOM adsorption isotherms on all carbons are shown in Figure 5.6. The single-solute and preloading TCE isotherms for individual carbons at the two preloading levels are shown in Figures 5.7 to 5.11.

The DOM uptake was in the order of  $F400He \approx HD4000ST > OLC \approx CRC \gg ACF10$  (Figure 5.6). The minimal DOM uptake demonstrated by ACF10 was consistent

with the observations of previous research that the pores  $<10 \text{ \AA}$  are not accessible to DOM molecules (Pelekani and Snoeyink, 2000; Cheng et al, 2005). This finding further supports that  $10 \text{ \AA}$  can be an important pore size cutoff to examine the DOM-SOC competitions. OLC and CRC, despite their microporous nature, showed similar but low degree of DOM uptakes, indicating that some DOM molecules can access pores of  $10\text{-}20 \text{ \AA}$  since these two carbons had small pore volumes in pores  $>20 \text{ \AA}$ . F400He and HD4000ST showed similar but significantly higher degree of DOM uptakes than the other three adsorbents. Despite the significantly higher pore volume of HD4000ST in pores  $>20 \text{ \AA}$  than F400He, they exhibited similar DOM uptakes. It is difficult to assign precise boundaries for the optimum adsorption pore size region for the DOM due to its heterogeneous molecular size distribution. HD4000ST had one unit lower  $\text{pH}_{\text{PZC}}$  than F400He. Although it is known that DOM adsorption decreases with increasing carbon surface acidity (Karanfil and Kilduff, 1999), it has been shown that one unit difference in the  $\text{pH}_{\text{PZC}}$  in the basic pH range is less likely to be the primary factor affecting the DOM adsorption (Cheng et al., 2005). These observations also suggest that there is an overlap in the optimum adsorption pore size region of atrazine and that of some of the DOM components used in this study.

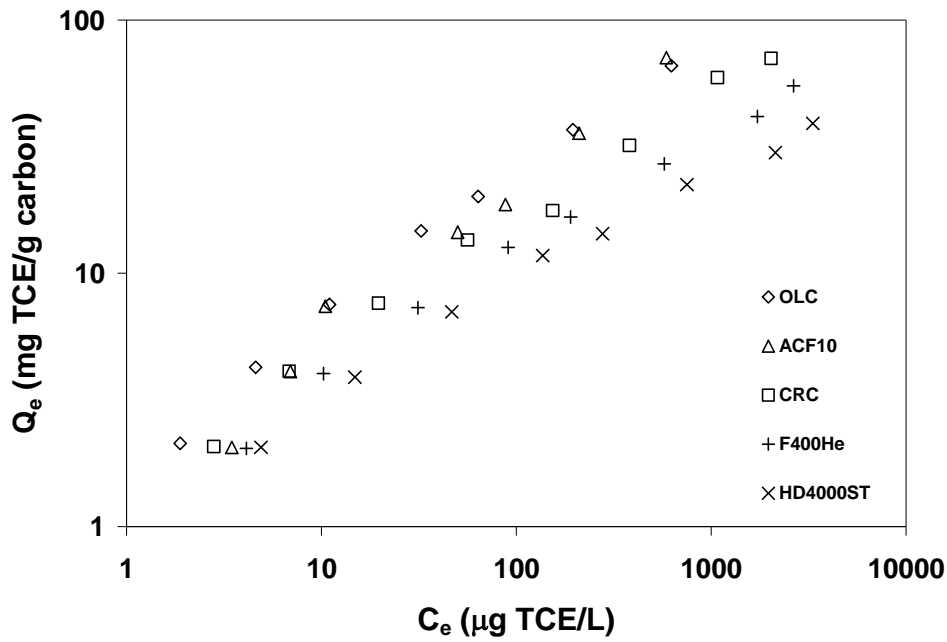


Figure 5.4 TCE adsorption isotherms for carbons preloaded with 5 mg DOC/L

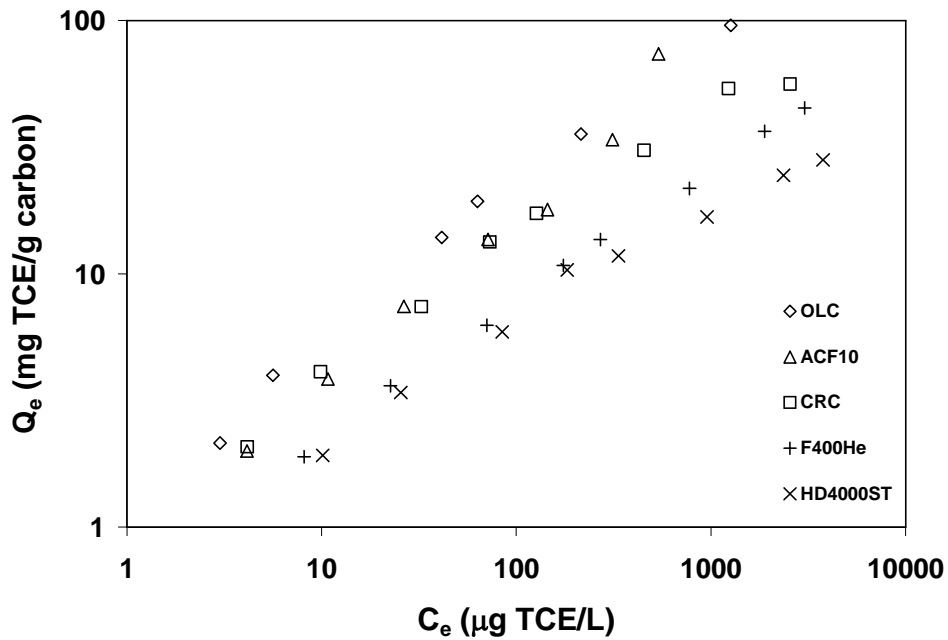


Figure 5.5 TCE adsorption isotherms for carbons preloaded with 20 mg DOC/L

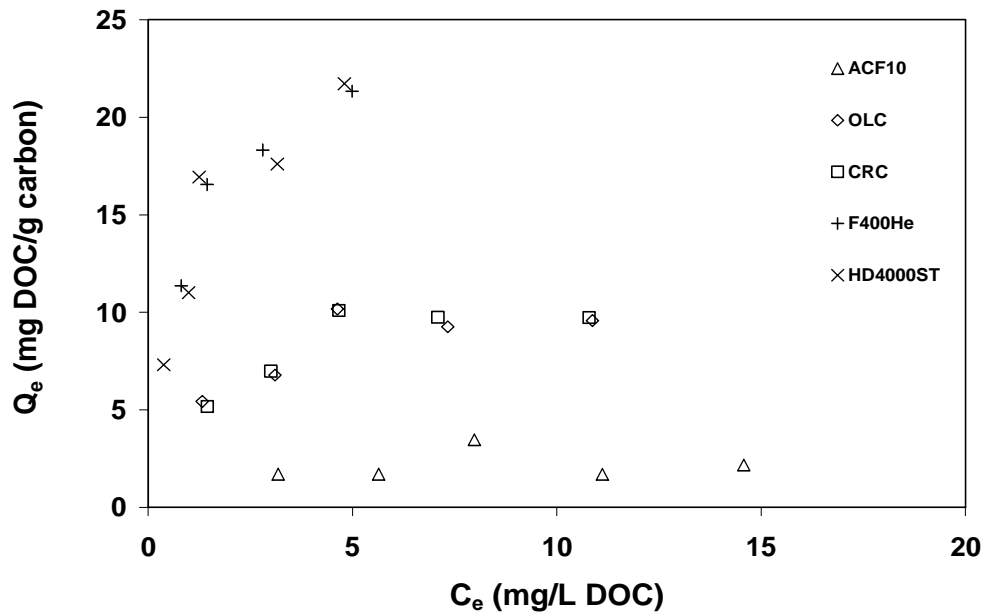


Figure 5.6 Single solute DOM isotherms for all carbons

The TCE isotherm data for all the carbons were modeled using the Freundlich equation:

$$q_e = K_F C_e^n$$

$q_e$  = solid-phase equilibrium concentration, mg/g

$C_e$  = aqueous phase equilibrium concentration,  $\mu\text{g/L}$

$K_F$  = Freundlich equilibrium capacity parameter providing a measure of overall adsorption capacity.

$n$  = exponential parameter relating to the magnitude of the driving force for the adsorption and the distribution of adsorption site energies (Weber, 1972).

The Freundlich parameters  $K_F$  and  $n$  were determined by linear geometric mean functional regression of log-transformed experimental data (Smith and Weber, 1989; Halfon, 1985; Olmstead and Weber, 1990). The single solute and preloading isotherms of individual carbons and the corresponding Freundlich fits are presented in Figures 5.7 to 5.11 and the Freundlich parameters are summarized in Table 5.2. The 95 % confidence intervals for the Freundlich parameters was calculated as is shown in Table A1 in the appendix.

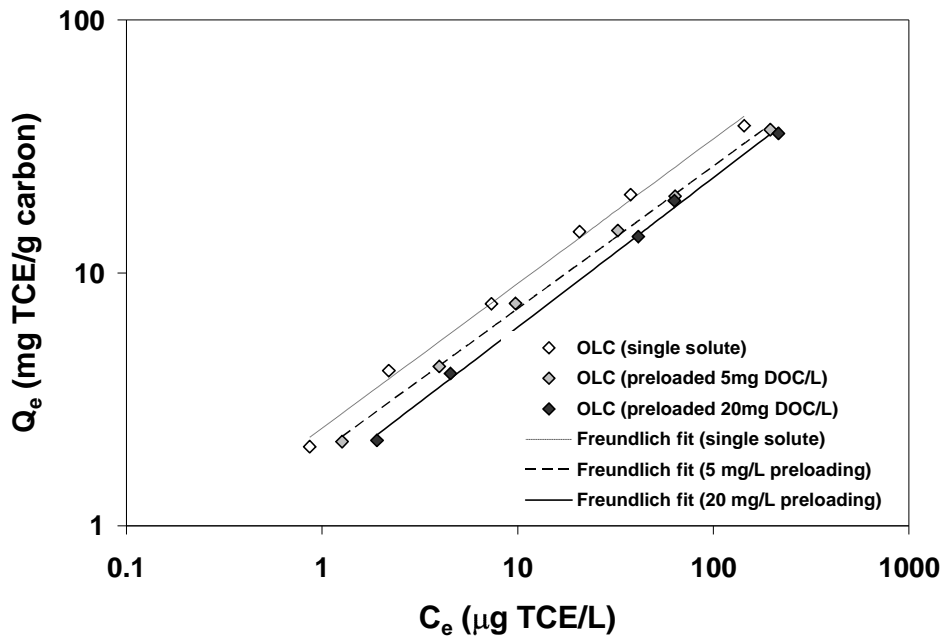


Figure 5.7 TCE single solute and preloading isotherms for OLC

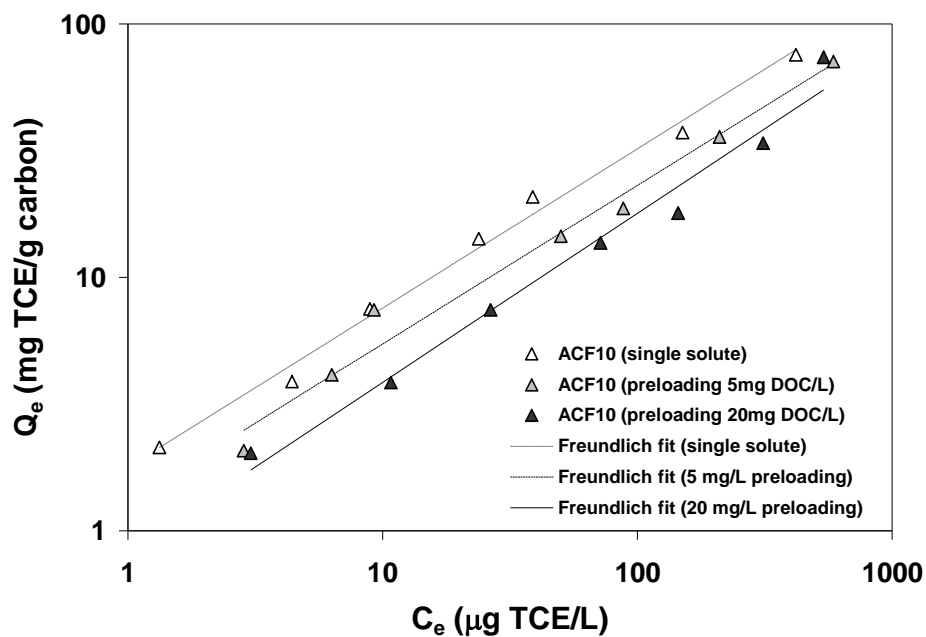


Figure 5.8 TCE single solute and preloading isotherms for ACF10

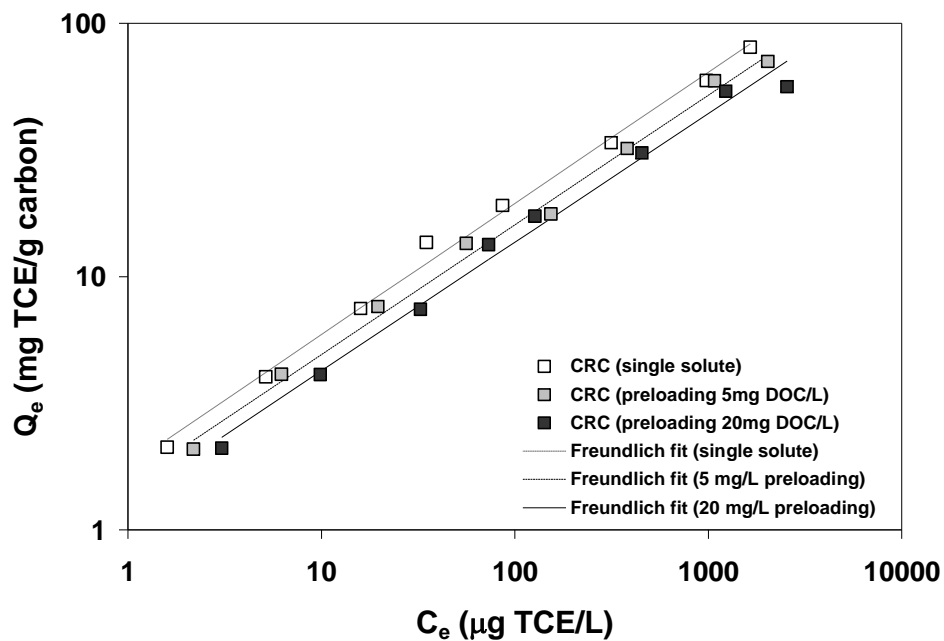


Figure 5.9 TCE single solute and preloading isotherms for CRC

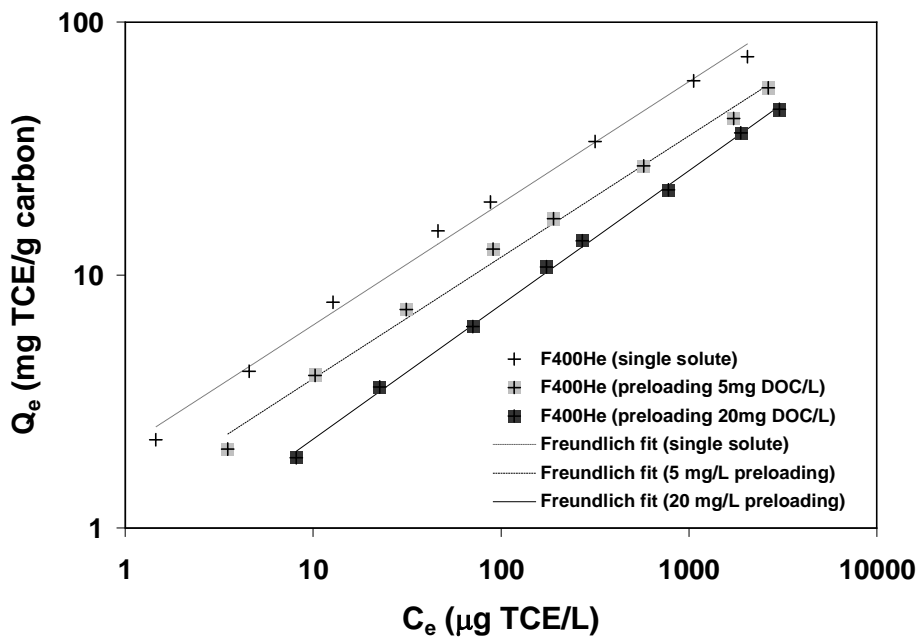


Figure 5.10 TCE single solute and preloading isotherms for F400He

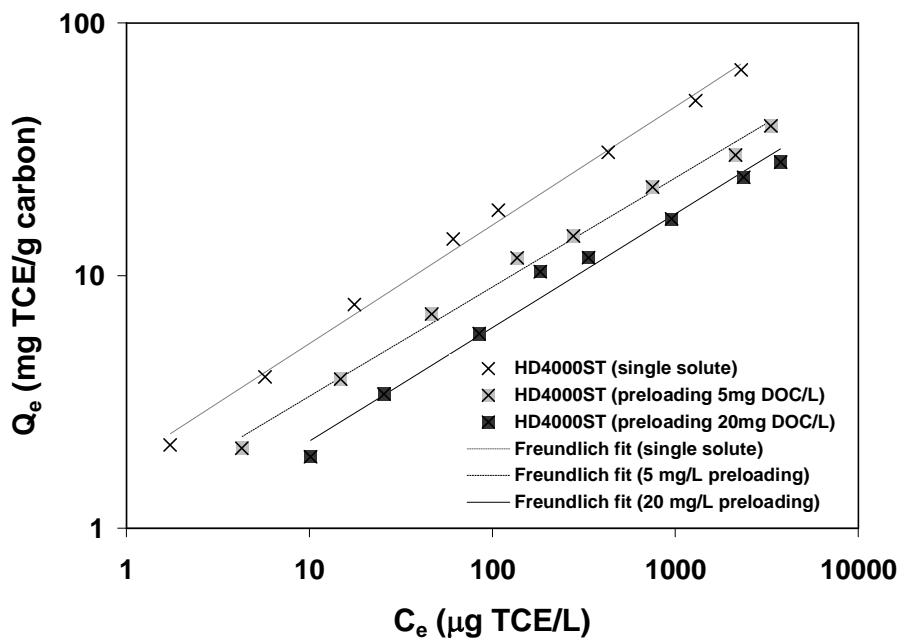


Figure 5.11 TCE single solute and preloading isotherms for HD4000ST

Table 5.2 Freundlich coefficients for all TCE adsorption isotherms

| <b>Isotherm</b>                          | <b><math>K_F</math></b> | <b><math>N</math></b> |
|--|-------------------------|-----------------------|
| <b>OLC</b> (single solute)               | 2.43                    | 0.57                  |
| <b>OLC</b> (preloading 5 mg DOC/L)       | 1.97                    | 0.58                  |
| <b>OLC</b> (preloading 20 mg DOC/L)      | 1.56                    | 0.59                  |
| <b>ACF10</b> (single solute)             | 1.78                    | 0.62                  |
| <b>ACF10</b> (preloading 5 mg DOC/L)     | 1.30                    | 0.62                  |
| <b>ACF10</b> (preloading 20 mg DOC/L)    | 0.78                    | 0.66                  |
| <b>CRC</b> (single solute)               | 1.79                    | 0.51                  |
| <b>CRC</b> (preloading 5 mg DOC/L)       | 1.51                    | 0.51                  |
| <b>CRC</b> (preloading 20 mg DOC/L)      | 1.32                    | 0.51                  |
| <b>F400He</b> (single solute)            | 2.10                    | 0.48                  |
| <b>F400He</b> (preloading 5 mg DOC/L)    | 1.29                    | 0.48                  |
| <b>F400He</b> (preloading 20 mg DOC/L)   | 0.66                    | 0.53                  |
| <b>HD4000ST</b> (single solute)          | 1.83                    | 0.47                  |
| <b>HD4000ST</b> (preloading 5 mg DOC/L)  | 1.20                    | 0.44                  |
| <b>HD4000ST</b> (preloading 20 mg DOC/L) | 0.78                    | 0.45                  |

Pore blockage is due to the adsorption of DOM molecules at the pore entrances. If large enough DOM molecules are adsorbed at the pore entrances, it is likely that the steric hindrances caused by the protrusion of these molecules into the bulk solution would hamper the diffusion of target SOC further into the pore. This results in the surface sites deeper in the pore remaining unoccupied or becoming inaccessible to the target SOC molecules. Pore blockage does not change the energy distribution of the adsorption sites but only their availability to the target SOC molecules. Therefore, as a result of preloading the  $n$  value would remain approximately constant, while the value of  $K_F$  would decrease (Carter et al., 1992). This also means pore blockage would result in the parallel shift of the Freundlich isotherms of target solute in downward direction. This corresponds to the observations in this study: the isotherms of each carbon under the three different experimental conditions (single solute and the two preloading conditions) showed parallel shifts. Therefore, it appears that preadsorbed DOM blocked the carbon pores leading to the sites of TCE adsorption. This is also consistent with the different adsorption regions of TCE and DOM molecules, where TCE primarily adsorbs in pores less than 10 Å, whereas DOM adsorb in pores >10 Å.

To further examine the impact of DOM preloading, the reduction degree of TCE uptake was calculated at three different concentration levels of the isotherms, 10, 100 and 500 µg/L, using the TCE uptakes at a particular preloading level and that in distilled and deionized water (Table 5.3). Since the preloading effect resulted in parallel shifts of the isotherms, the percent reductions in the TCE uptakes were independent of equilibrium concentration. The reduction degree of the TCE uptakes of the three microporous carbons

(i.e., OLC, CRC and ACF10) was significantly lower than those of F400He and HD4000ST. In addition, the impact of preloading effect (i.e., the percent reduction in TCE uptake) increased more severely with increasing background DOM concentration for F400He and HD4000ST than OLC, CRC and ACF10. These observations were related to the significantly higher DOM uptakes of F400He and HD4000ST than OLC, CRC and ACF10 (Figure 5.6). It appears that the preloaded DOM, which increased with the increase in DOM concentration of preloading solution, blocked the pores for TCE adsorption and resulting in the parallel shift of the Freundlich isotherms.

Among the three most microporous adsorbents, OLC, CRC and ACF10, the preloading effect was similar for OLC and CRC, which was lower than that observed for ACF10, despite OLC showing higher DOM uptake than CRC. This suggests that pore structure exerts additional impact on the DOM-SOC competition. It appears that DOM molecules, despite their low degree of adsorption, block more effectively and/or a higher number of ACF pores than those of OLC and CRC. Overall, these results extend the previous findings of Karanfil et al. (2006) with carbon fibers to GACs showing that for the SOC molecules that adsorb primarily in pores  $<10 \text{ \AA}$ , highly microporous GACs (i.e., activated carbons having high pores volumes in less than  $10 \text{ \AA}$  and minimal volumes in pores  $>10 \text{ \AA}$ ) gives the best results for controlling DOM competition. The TCE isotherms under two preloading conditions showed that OLC and ACF10 exhibited the highest TCE uptakes, and the difference between the TCE uptakes of these carbons and those of F400He and HD4000ST increased with increasing preloading DOM concentration (Figures 5.4 and 5.5).

These results strongly suggest that pore blockage is the dominant competing mechanism of DOM on the adsorption of a pollutant with small molecular size like TCE adsorbing in the primary micropore size region ( $<10 \text{ \AA}$ ), which is inaccessible to the bulky DOM molecules. The equilibrium data also indicates that the best way to alleviate this DOM competition is to use an extremely microporous carbon having narrow pore size distribution and with most of its pore volume in the pore size region of less than  $10 \text{ \AA}$  (i.e., the target pore size region of target SOC). Such carbon can selectively adsorb the target SOC from the solution and drastically reduce the SOC-DOM competition.

Table 5.3 Reduction in TCE uptake at the two preloading conditions

| Activated Carbon | Preloading | % reduction in TCE uptake |          |          |
|------------------|------------|---------------------------|----------|----------|
|                  |            | 10 µg/L                   | 100 µg/L | 500 µg/L |
| <b>OLC</b>       | 5 mg/L     | 20.4                      | 21.9     | 22.9     |
|                  | 20 mg/L    | 32.8                      | 29.6     | 27.3     |
| <b>ACF10</b>     | 5 mg/L     | 27.7                      | 28.2     | 28.6     |
|                  | 20 mg/L    | 49.1                      | 44.4     | 40.8     |
| <b>CRC</b>       | 5 mg/L     | 16.6                      | 17.7     | 18.5     |
|                  | 20 mg/L    | 28.1                      | 29.7     | 30.9     |
| <b>F400He</b>    | 5 mg/L     | 38.7                      | 38.8     | 38.9     |
|                  | 20 mg/L    | 64.6                      | 60.3     | 57.0     |
| <b>HD4000ST</b>  | 5 mg/L     | 38.1                      | 43.1     | 46.4     |
|                  | 20 mg/L    | 59                        | 60.7     | 61.7     |

### 5.2.3 Atrazine isotherms

Single solute atrazine adsorption isotherms of all carbons are shown in Figure 5.12. The atrazine uptake of F400He was the highest and followed by CRC  $\approx$  HD4000ST > OLC >> ACF10.

In the pore size range of 10 to 20 Å, F400He has the highest available pore volume (0.13cm<sup>3</sup>/g) followed by CRC and HD4000ST with similar pore volumes

(0.11cm<sup>3</sup>/g) (Table 5.1). On the other hand, OLC has significantly less pore volume (0.06cm<sup>3</sup>/g) in this pore size region and that of ACF10 is the lowest (0.02cm<sup>3</sup>/g). Therefore, there is a trend between the atrazine adsorption capacities of the carbons and their pore volume available in 10 to 20 Å pore size region. This observation is in agreement with previous research results that adsorption of atrazine occurs in 8 to 20 Å pore size range (Pelekani and Snoeyink, 2000, 2001).

Atrazine adsorption by the five activated carbons was also investigated under two DOM preloading conditions (5 and 20 mg DOC/L). The preloading isotherms are presented in Figure 5.13 and 5.14, respectively. The results indicate that for all carbons studied, DOM preloading reduced the atrazine adsorption capacities. The extent of reduction in adsorption capacity was greater at the preloading of 20 mg DOC/L than of 5 mg DOC/L. The DOM preloading concentration, however, did not change the relative adsorption capacities of these carbons.

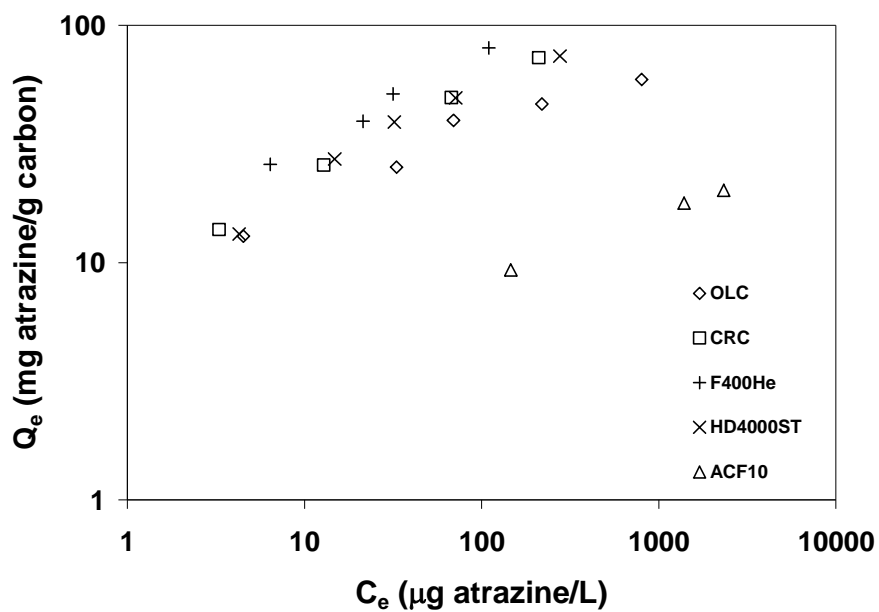


Figure 5.12 Single solute atrazine adsorption isotherms

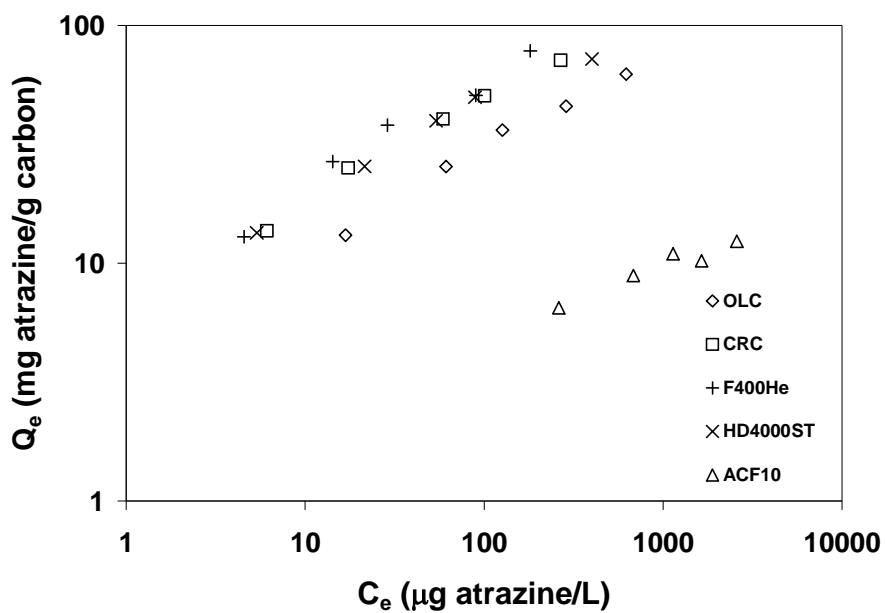


Figure 5.13 Atrazine adsorption isotherms for carbons preloaded with 5 mg DOC/L

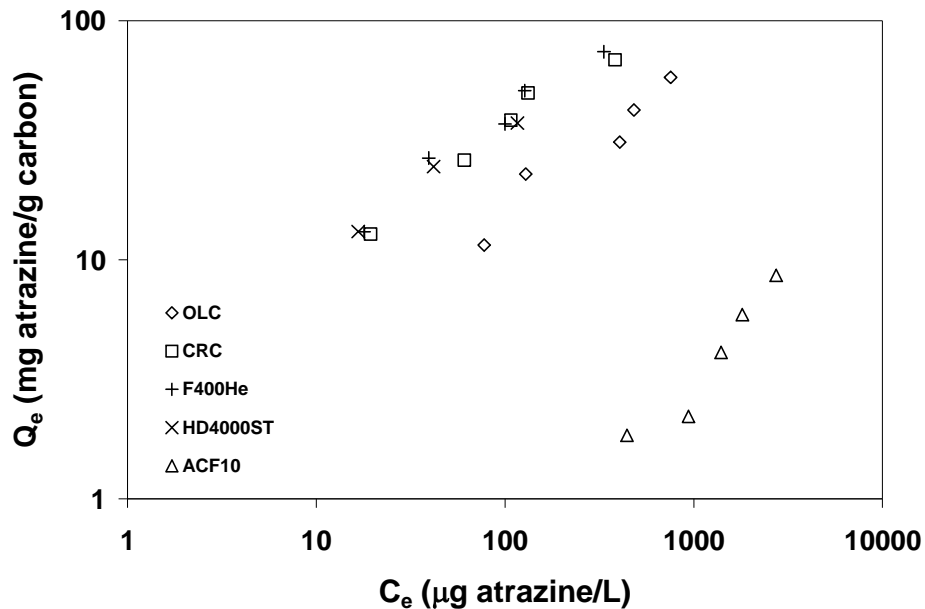


Figure 5.14 Atrazine adsorption isotherms for carbons preloaded with 20 mg DOC/L

The results indicate that the carbons most affected by the DOM preloading were the microporous carbons: ACF10 and OLC. The carbons with a broader pore size distribution (F400He, CRC, and HD4000ST), ranging from primarily microporous to a large volume of secondary micropores and some mesopores, exhibited some reduction in their adsorption capacities, but to a much lesser extent than the microporous carbons (ACF10 and OLC). These findings are in agreement with those of Pelekani and Snoeyink (1999), which showed that the atrazine adsorption of microporous activated carbon fiber ACF10 was more severely impacted by DOM preloading than that of the mesoporous activated carbon fiber ACF25. This is more evident in the single solute and preloading isotherms of individual carbons presented in Figures 5.16 to 5.19.

The single solute and preloading isotherms of individual carbon were also modeled using the Freundlich equation. The isotherms and the corresponding Freundlich fits are shown from Figures 5.16 to 5.19, and the corresponding Freundlich coefficients are listed in Table 5.3. The 95 % confidence intervals for the Freundlich parameters are not shown in the text since due to the use of radio-labeled compound only 3 to 5 points were available on the isotherms and it would not be statistically meaningful to compare such a small data set.

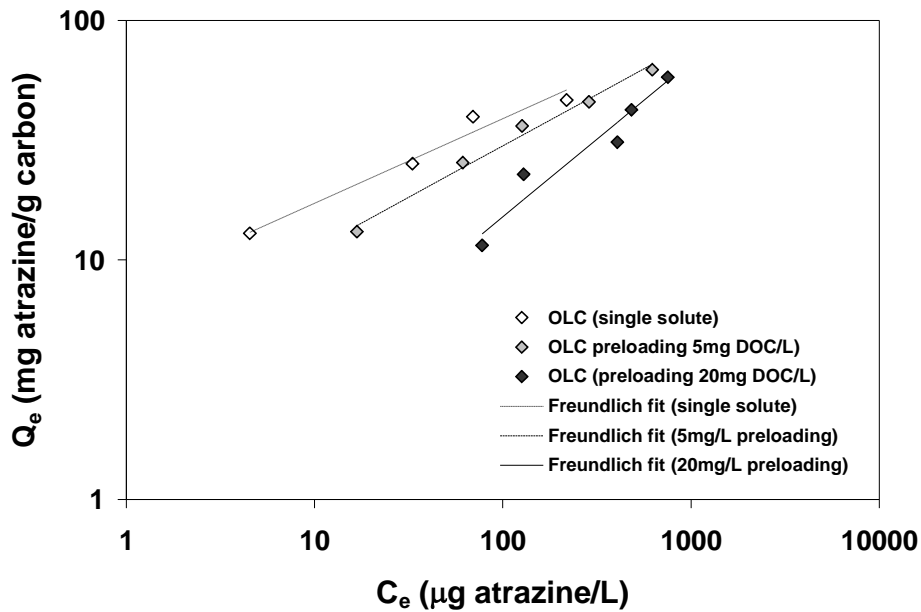


Figure 5.15 Atrazine single solute and DOM preloading isotherms for OLC

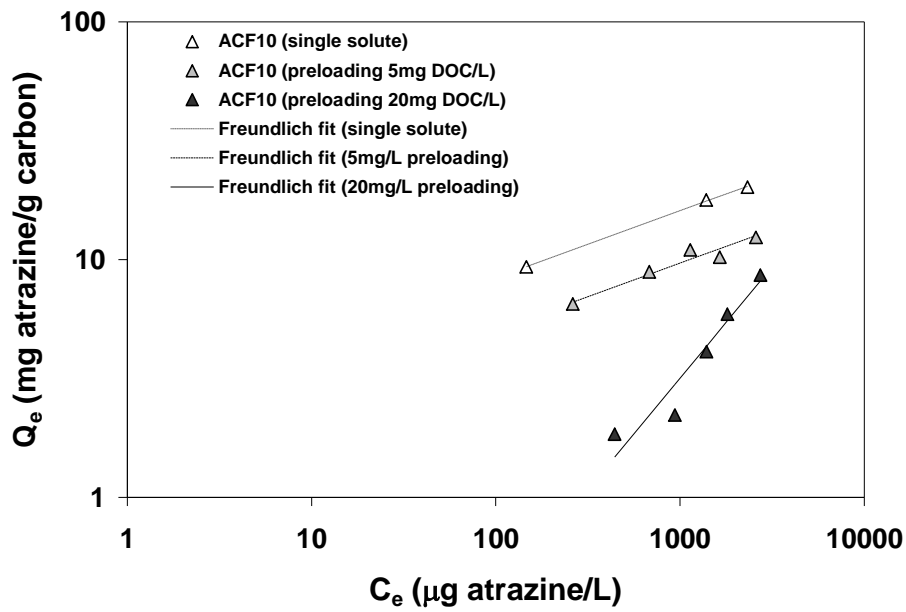


Figure 5.16 Atrazine single solute and DOM preloading isotherms for ACF10

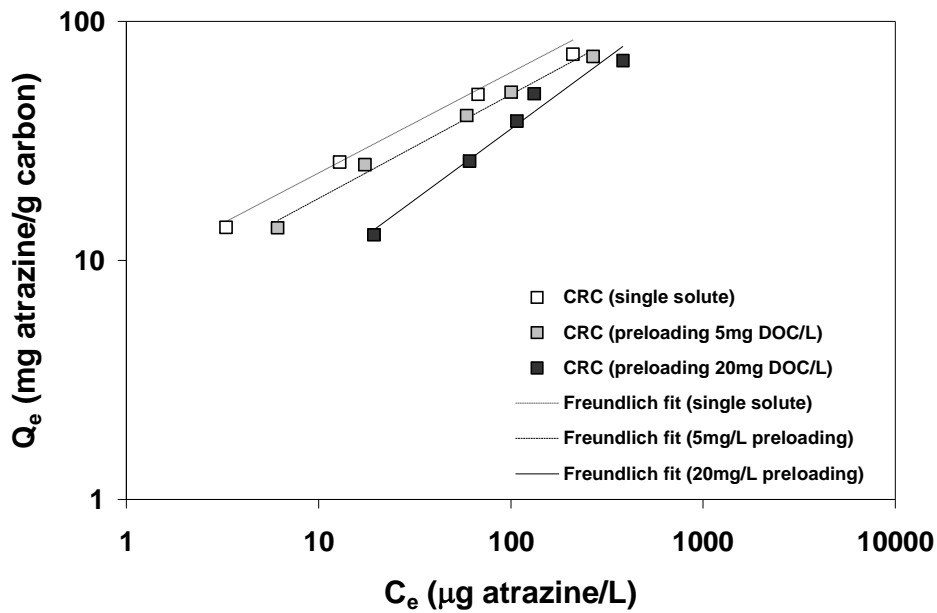


Figure 5.17 Atrazine single solute and DOM preloading isotherms for CRC

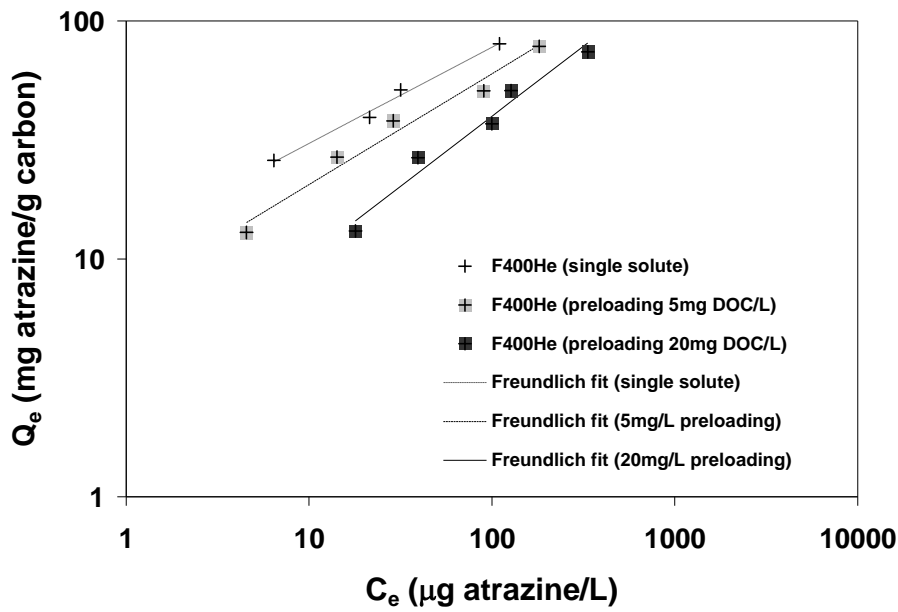


Figure 5.18 Atrazine single solute and DOM preloading isotherms for F400He

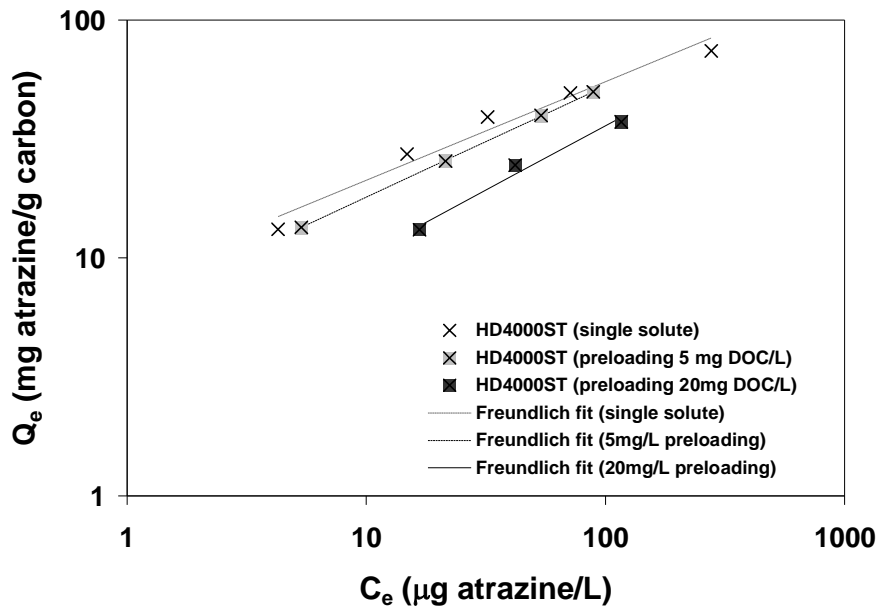


Figure 5.19 Atrazine single solute and DOM preloading isotherms for HD4000ST

Table 5.4 Freundlich coefficients for atrazine adsorption isotherms

| <b>Isotherm</b>                          | <b><math>K_F</math></b> | <b><math>N</math></b> |
|--|-------------------------|-----------------------|
| <b>OLC</b> (single solute)               | 7.68                    | 0.35                  |
| <b>OLC</b> (preloading 5 mg DOC/L)       | 4.15                    | 0.43                  |
| <b>OLC</b> (preloading 20 mg DOC/L)      | 0.76                    | 0.65                  |
| <b>ACF10</b> (single solute)             | 2.28                    | 0.26                  |
| <b>ACF10</b> (preloading 5 mg DOC/L)     | 1.39                    | 0.28                  |
| <b>ACF10</b> (preloading 20 mg DOC/L)    | 0.01                    | 0.93                  |
| <b>CRC</b> (single solute)               | 8.84                    | 0.42                  |
| <b>CRC</b> (preloading 5 mg DOC/L)       | 6.70                    | 0.44                  |
| <b>CRC</b> (preloading 20 mg DOC/L)      | 2.33                    | 0.59                  |
| <b>F400He</b> (single solute)            | 12.08                   | 0.40                  |
| <b>F400He</b> (preloading 5 mg DOC/L)    | 7.03                    | 0.47                  |
| <b>F400He</b> (preloading 20 mg DOC/L)   | 2.65                    | 0.59                  |
| <b>HD4000ST</b> (single solute)          | 8.17                    | 0.41                  |
| <b>HD4000ST</b> (preloading 5 mg DOC/L)  | 6.11                    | 0.47                  |
| <b>HD4000ST</b> (preloading 20 mg DOC/L) | 2.99                    | 0.54                  |

During preloading experiments, when DOM components reach the carbon surface first, they occupy the higher-energy sites. This results in a decrease in the number of higher energy sites available for SOC adsorption. This competitive adsorption phenomenon is reflected by a decrease in the Freundlich capacity coefficient  $K_F$  and an increase in the value of the Freundlich exponent  $n$  relative to that obtained in single-solute adsorption (Carter et al., 1992). This change in the Freundlich parameters leads to a downward non-parallel shift of the isotherms. Reduction in the value of  $K_F$  signifies a reduction in the total number of adsorption sites available for the SOC adsorption and an increase in the Freundlich exponent  $n$  signifies that the energy distribution of adsorption sites available are of a more homogeneous nature. The Freundlich coefficient for atrazine adsorption isotherms followed the pattern explained above. With increasing DOM preloading, the  $K_F$  values decreased and the corresponding  $n$  values increased (Table 5.4). As a result, the percent reduction in atrazine uptake increased with decreasing equilibrium concentration (Table 5.5). This isotherm behavior indicates that the occurrence of site competition is a more important mechanism than pore blockage on atrazine adsorption under the DOM conditions (Carter et al., 1992).

In contrast to TCE, for the atrazine adsorption, the carbons (e.g., F400He and HD4000ST) with a broader pore size distribution ranging from primarily microporous to a large volume of secondary micropores and some mesopores exhibited a much less reduction in their adsorption capacities than the microporous carbons (ACF10 and OLC). The density of atrazine at 25°C is 1.19 g/mL, therefore atrazine molecules occupy approximately 0.09 cm<sup>3</sup>/g carbon at the highest surface loadings, ~ 100 mg atrazine/g

carbon, observed in this study. ACF10 only had 0.03 cm<sup>3</sup>/g volume in pores 10-20 Å and none in pores >20 Å. As a result, ACF10 showed the lowest atrazine uptake in the single solute isotherms and suffered the most from preloading effects (Tables 5.4 and Table 5.5). These results also indicated that there are DOM components that adsorb in 10-20 Å pore region and strongly compete with the atrazine. OLC had only 0.07 cm<sup>3</sup>/g volume in the 10-20 Å pore size region and 0.02 cm<sup>3</sup>/g in pores >20 Å. This was just about the total volume needed to accommodate the atrazine molecules. As a result, OLC showed the second most significant reduction in the atrazine uptake after ACF10. The other three carbons, CRC, F400He, HD4000ST showed similar uptakes under the two preloading conditions tested (Figures 5.13 and 5.14). One characteristic common of these carbons is that they all had similar pore volume in the 10-20 Å region (Table 5.1). However, it was clearly noted that CRC showed significantly lower DOM uptake than F400He and HD4000ST since the former is more microporous than the latter. Therefore, one possible explanation for the observed trend is that despite the difference in the overall DOM uptakes of these carbons, the amount of DOM adsorbed in the 10-20 Å region was comparable at each preloading condition, as a result the atrazine adsorption by these three preloaded carbon showed comparable uptakes. It should also be noted that in single solute adsorption experiments, OLC, F400He and HD4000ST showed similar atrazine adsorption despite the difference in their pore size distribution, confirming the importance of 10-20 Å for the adsorption of this SOC. Similar uptakes of these carbons under preloading conditions suggest that the major competition between atrazine and DOM components was occurring in the 10-20 Å pore region. It is, however, noteworthy

that the DOM adsorption by CRC, although small, did not result in pore blockage effect for the subsequent atrazine adsorption. For example, adsorption of a very small amount of DOM by ACF10 resulted in significant reduction in the TCE uptake. This appears to be related to the pore structure of CRC and packing of DOM in the CRC. The findings with CRC were interesting because the postulated hypothesis was that using an activated carbon with broad pore size distribution (i.e., mesoporous) would reduce the DOM-SOC competition for a SOC with optimum adsorption region of pore size larger than 10 Å. Although this hypothesis was validated by the results of F400He and HD4000ST, the results obtained with CRC suggest that a carbon with narrow pore size distribution can also show low degree of DOM-SOC competition effect, thus high SOC uptake, if it has high volume in the optimum adsorption pore region of SOC, and DOM adsorption does not result in major pore blockage effect. The observation with CRC maybe viewed as an exception but it indicates that further research regarding the effect of pore structure on SOC-DOM competitions is warranted.

Table 5.5: Reduction in Atrazine uptake at the two preloading conditions

| Activated Carbon | Preloading | % reduction in Atrazine uptake |          |          |
|------------------|------------|--------------------------------|----------|----------|
|                  |            | 10 µg/L                        | 100 µg/L | 500 µg/L |
| <b>OLC</b>       | 5 mg/L     | 35.5                           | 23.0     | 12.9     |
|                  | 20 mg/L    | 80.4                           | 61.1     | 37.3     |
| <b>ACF10</b>     | 5 mg/L     | 39.5                           | 39.6     | 39.7     |
|                  | 20 mg/L    | 99.0                           | 95.6     | 87.4     |
| <b>CRC</b>       | 5 mg/L     | 21.7                           | 19.1     | 17.3     |
|                  | 20 mg/L    | 60.9                           | 41.9     | 23.4     |
| <b>F400He</b>    | 5 mg/L     | 32.9                           | 22.6     | 14.5     |
|                  | 20 mg/L    | 66.5                           | 48.8     | 31.2     |
| <b>HD4000ST</b>  | 5 mg/L     | 15.3                           | 4.1      | -4.6     |
|                  | 20 mg/L    | 51.2                           | 34.8     | 20.2     |

### 5.3 TCE adsorption kinetics

Adsorption by activated carbon is described as a four stage process. The first step is the bulk diffusion of the SOC in the aqueous phase followed by film diffusion at the activated carbon surface. The third step is intraparticle diffusion (pore diffusion and/or surface diffusion) within the adsorbent pores and finally, the adsorption of the adsorbate on target adsorption sites. The final adsorption step is assumed to be instantaneous and in

completely mixed batch systems bulk diffusion is usually not a limiting factor. Therefore, the rate limiting step is either film diffusion or intraparticle diffusion, or a combination of both (Baup et al., 2000). Since all GACs used in this study were of the same particle size range, it is expected that the effect of film diffusion for all the carbons on the adsorption of both SOC and DOM should be similar. Finally, it is important to note that ACF10 kinetics is not presented in this discussion since all the granular carbons were crushed and sieved to the same particle size range and the fiber on the other hand was cut in to fine pieces. The difference in particle size and shape makes it inappropriate to compare the adsorption kinetics of GACs and ACF10 in batch experiments. This section will therefore explore the kinetic behavior of the GACs and compare the adsorption kinetics of the four GACs with respect to their pore size distributions.

The adsorption kinetics of TCE was investigated in both single solute DDW experiments and in the presence of background DOM of 5 mg DOC/L. The single solute kinetics during the first 8 hours of contact time are presented in Figure 5.20. HD4000ST showed the fastest adsorption kinetics among all the GACs studied followed by F400He with slightly slower kinetic. Both HD4000ST and F400He showed faster kinetics than the microporous adsorbents OLC and CRC.

The superior kinetic behavior demonstrated by the mesoporous carbons (HD4000ST and F400He) over the microporous carbons (OLC and CRC) could be attributed to their open pore structure which seems to provide a kinetic advantage for the target TCE molecule to access the inner pore network. Therefore, lower TCE residual concentration in aqueous phase was obtained even though the TCE molecules may or

may not have reached its target adsorption sites. The concentration decay in liquid phase as a function of contacting time for all the carbons eventually levels off. Furthermore, it was observed that the kinetic plots for the microporous carbons eventually crossed that of the mesoporous carbons and the final equilibrium concentrations corresponded to those observed in the equilibrium isotherm experiments (Figure 5.21).

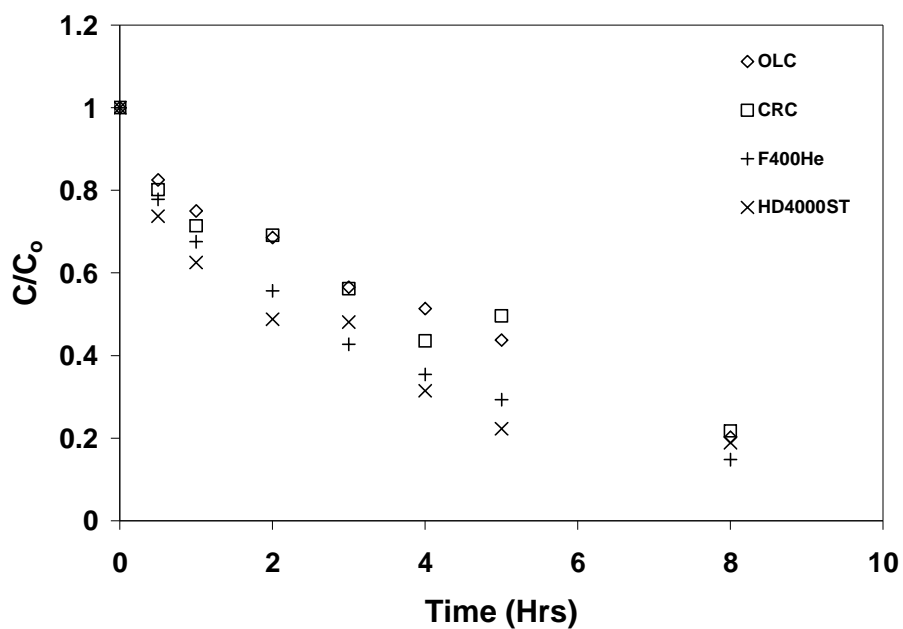


Figure 5.20. Single solute TCE adsorption kinetics (first 8 hours of contact time)

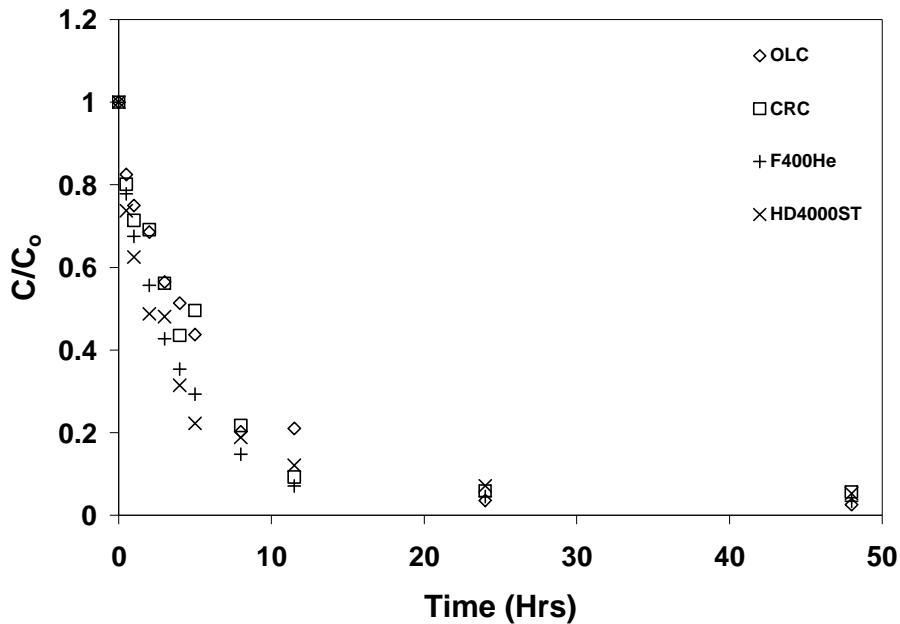


Figure 5.21 Single solute TCE adsorption kinetics (two days of contact time)

This suggests that even though the microporous carbons have the advantage of higher capacity over the mesoporous carbons, the trade off is the relatively slower adsorption kinetics to reach the final higher equilibrium capacity.

The TCE adsorption kinetics in the presence of 5 mg DOC/L background DOM showed that the concentration decay of all carbons showed very similar patterns (Figures 5.22 and 5.23), which is primarily due to the impact of DOM competition on the adsorption kinetics of the two mesoporous carbons. HD4000ST and F400He demonstrated slower TCE adsorption kinetics in the presence of DOM as compared to their single solute results (Figures 5.26 and 5.27, respectively); this was probably due to their open pore structures. The wide mesopores allow easier access of not just the TCE

molecule but also the background DOM components. The adsorption of DOM components in the secondary micropores and mesopores hinder the access of TCE molecules to the target micropore region. The microporous carbons (OLC and CRC) show insignificant adsorption to DOM molecules from the background aqueous solution due to the lack of pore volume in mesopore range. Consequently, the presence of DOM components exhibited little or no effect on the adsorption kinetics of TCE on microporous carbons (Figures 5.24 and 5.25), suggesting that the coverage of DOM on the external surface of carbon particle was not sufficient to hinder the diffusion of TCE molecules into the inner carbon pore network. This hypothesis is supported by the equilibrium isotherm results of the microporous carbons (OLC and ACF10), which show relatively little effect of DOM preloading.

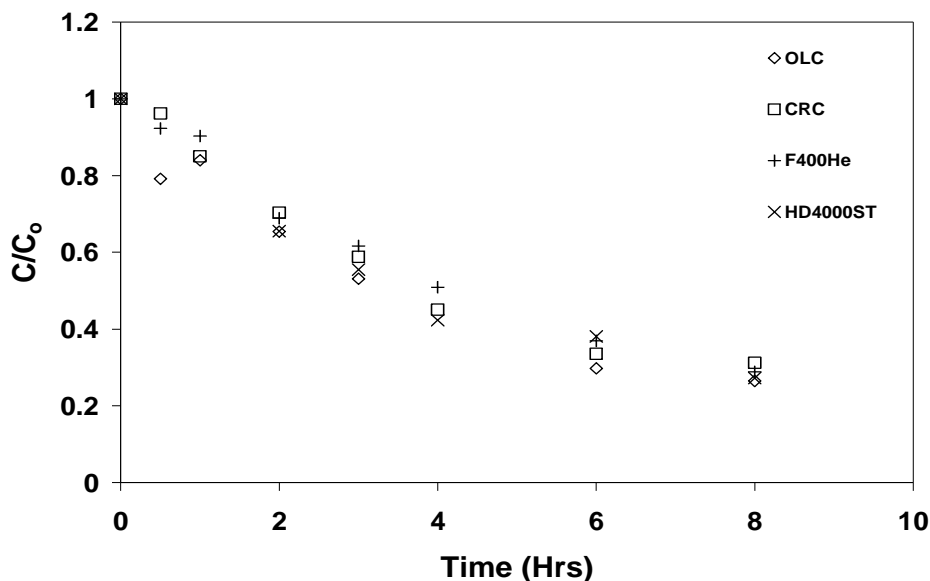


Figure 5.22 TCE adsorption kinetics in presence of background 5 mg DOC/L (first eight hours of contact time)

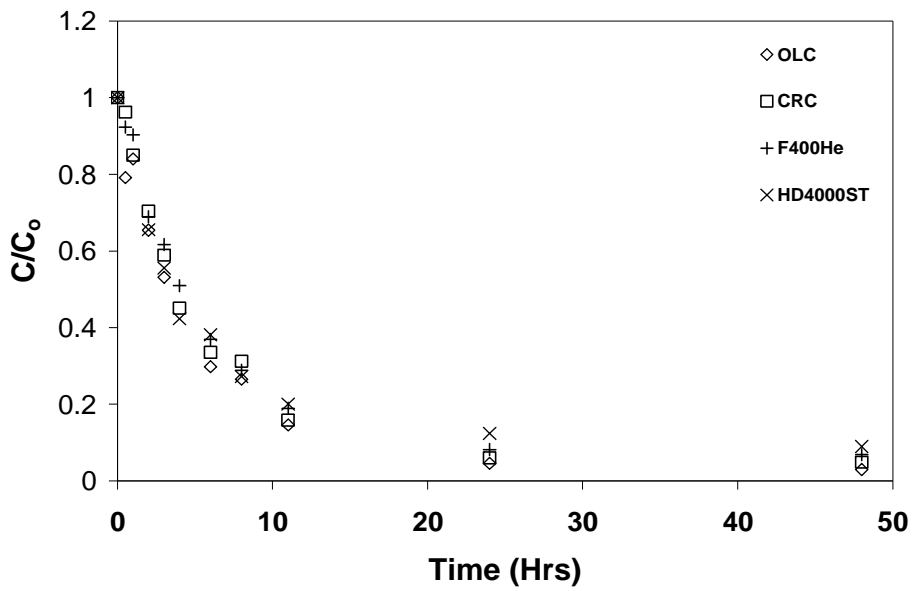


Figure 5.23 TCE adsorption kinetics in presence of background 5 mg DOC/L (two days of contact time)

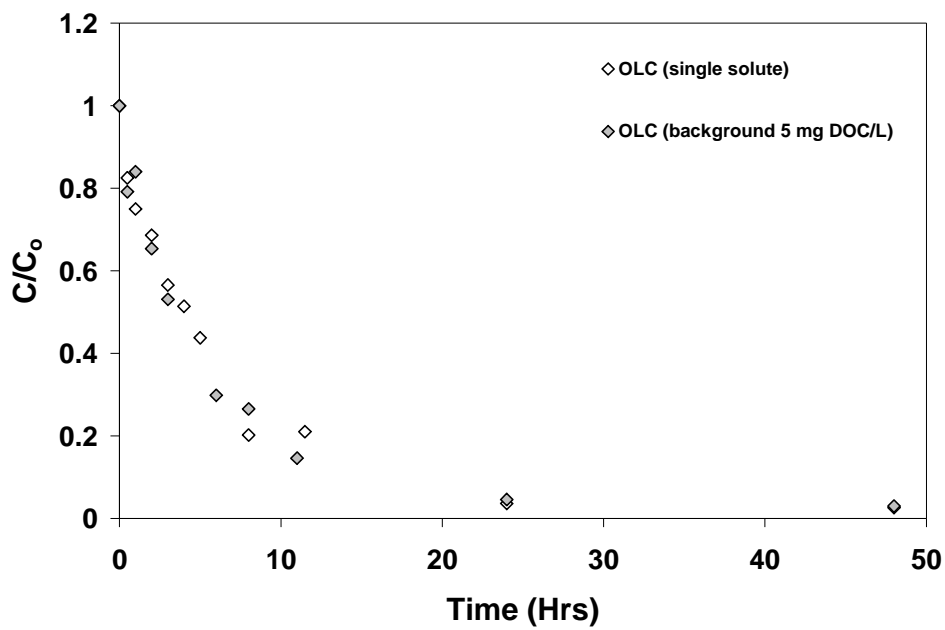


Figure 5.24 OLC kinetics for TCE adsorption (two days of contact time)

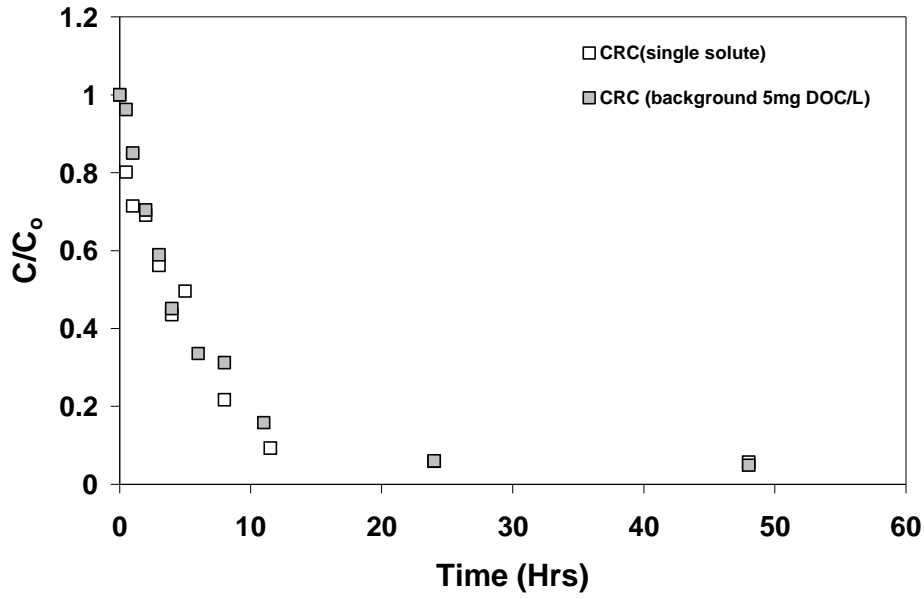


Figure 5.25 CRC kinetics for TCE adsorption (two days of contact time)

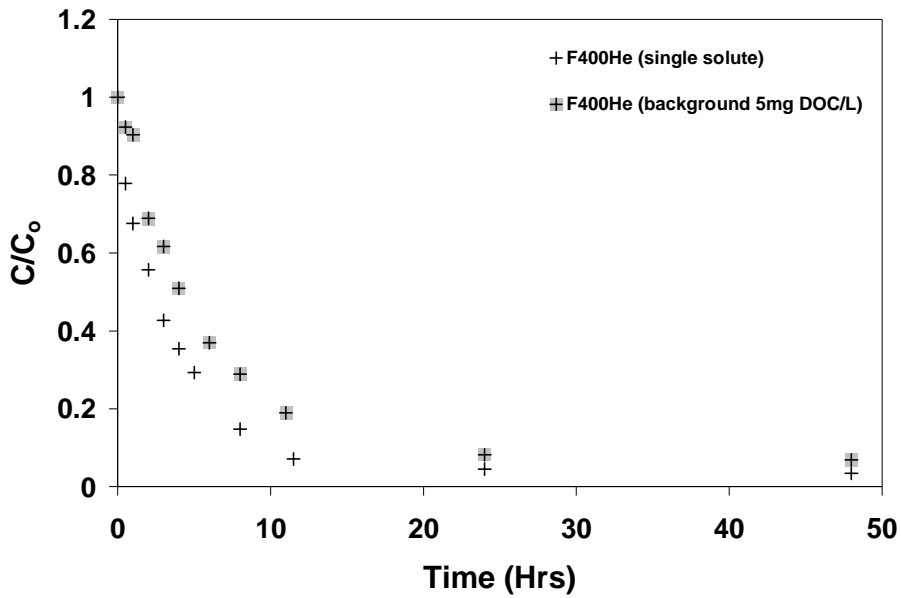


Figure 5.26 F400He kinetics for TCE adsorption (two days of contact time)

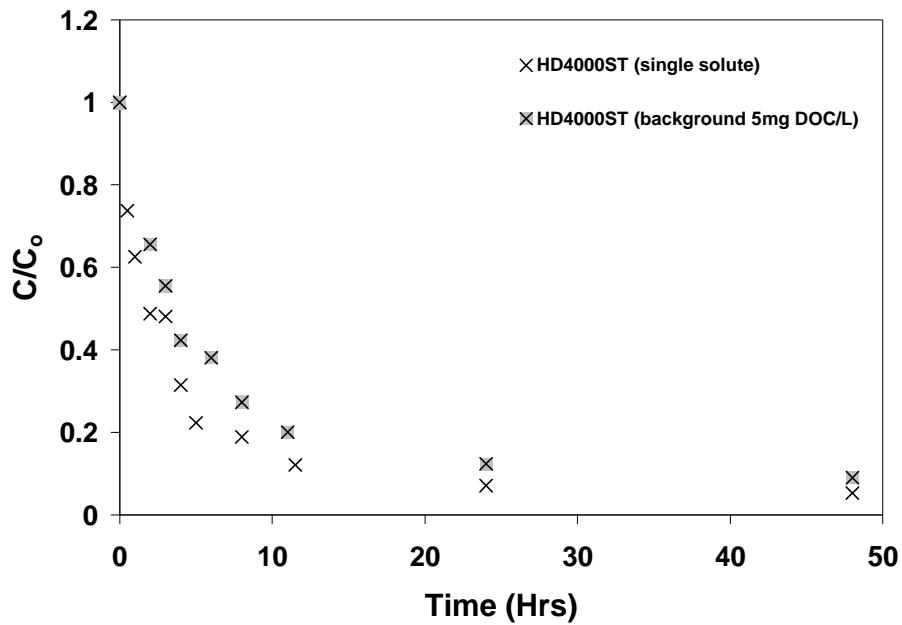


Figure 5.27 HD4000ST kinetics for TCE adsorption (two days of contact time)

#### 5.4 Atrazine adsorption kinetics

Atrazine adsorption kinetics was investigated on all the four GACs in DDW and in the presence of 5 mg DOC/L background DOM. The results of single solute atrazine adsorption kinetics during the first twelve hours of contact time for all GACs are shown in Figure 5.28.

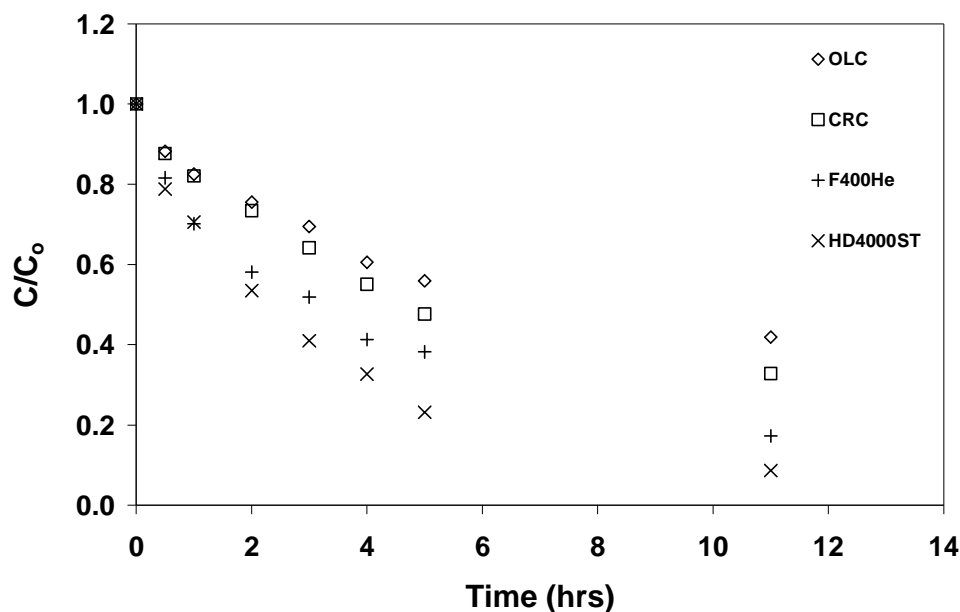


Figure 5.28 Single solute atrazine adsorption kinetics (twelve hours of contact time)

HD4000ST showed the fastest kinetics followed by F400He, CRC, and lastly OLC in DDW kinetics experiments (Figure 5.29). HD4000ST has the widest pore size distribution and maximum combined volume available in the secondary micropore and mesopore region. Therefore, just as in the case of TCE, it can be hypothesized that the wide pores allow faster and easier access of atrazine molecules to the inner carbon pore network. F400He has the largest volume in the target pore size region of atrazine (10-20 Å), thus it showed the highest atrazine uptake upon reaching equilibrium. However, the lower volume of F400He in pores >20 Å as compared to HD4000ST resulted in slower kinetics. The kinetic behaviors of CRC and OLC can subsequently be explained by extending the same argument with CRC showing slower kinetics than F400He for TCE

adsorption. OLC demonstrated the slowest kinetics amongst all the studied GACs. The final equilibrium concentrations of the carbons corresponded to the values in the isotherm experiments.

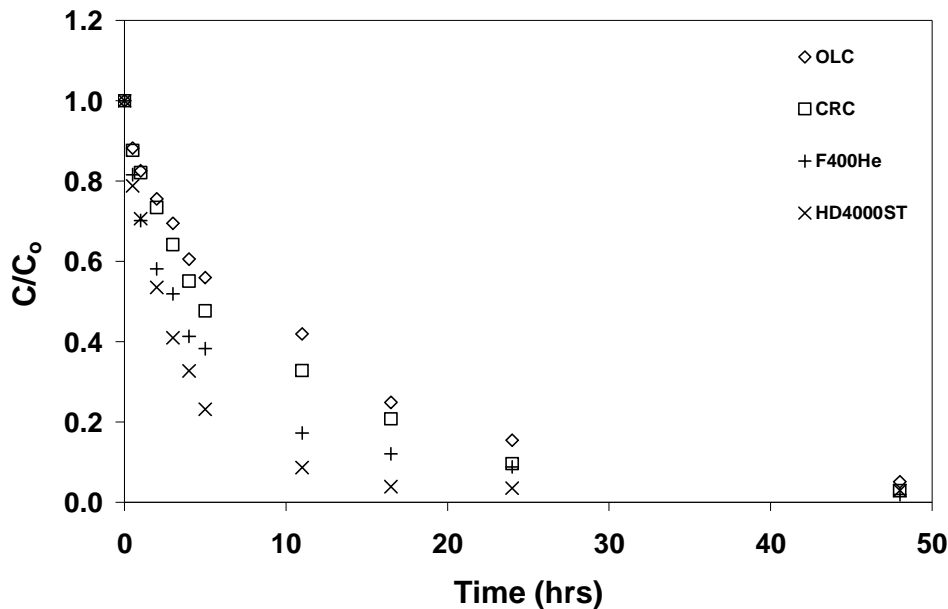


Figure 5.29 Single solute atrazine adsorption kinetics (two days of contact time)

The atrazine adsorption kinetics in the presence of 5 mg DOC/L background DOM for all GACs during the first twelve hours of contact time are shown in Figure 5.30. The atrazine adsorption kinetics on each carbon in the presence of 5gm DOC/L background DOM are shown in Figures 5.31 to 5.34. It is evident that as compared to their kinetics obtained under single solute condition, the competitive adsorption kinetics of the two microporous carbons are further separated from that of the two mesoporous carbons. This indicated that the presence of background DOM applies a definite negative

impact on the adsorption kinetics of microporous carbons. However, the DOM does not hinder atrazine adsorption on the mesoporous carbons. The open pore structure of the mesoporous carbons seems to be responsible for what observed, which is contrast to what demonstrated by the mesoporous carbons during TCE adsorption. This is probably because DOM, as mentioned earlier adsorbs in a wide pore size range, including the target adsorption region for atrazine. This kinetic data also suggests that if sufficient pore volume is available in the mesoporous carbons to accommodate both DOM and atrazine, the DOM preloading impact on the adsorption kinetics of atrazine is negligible. For the microporous carbons, the presence of DOM led to low atrazine adsorption rate due to the lack of pore volume required to accommodate both DOM and atrazine.

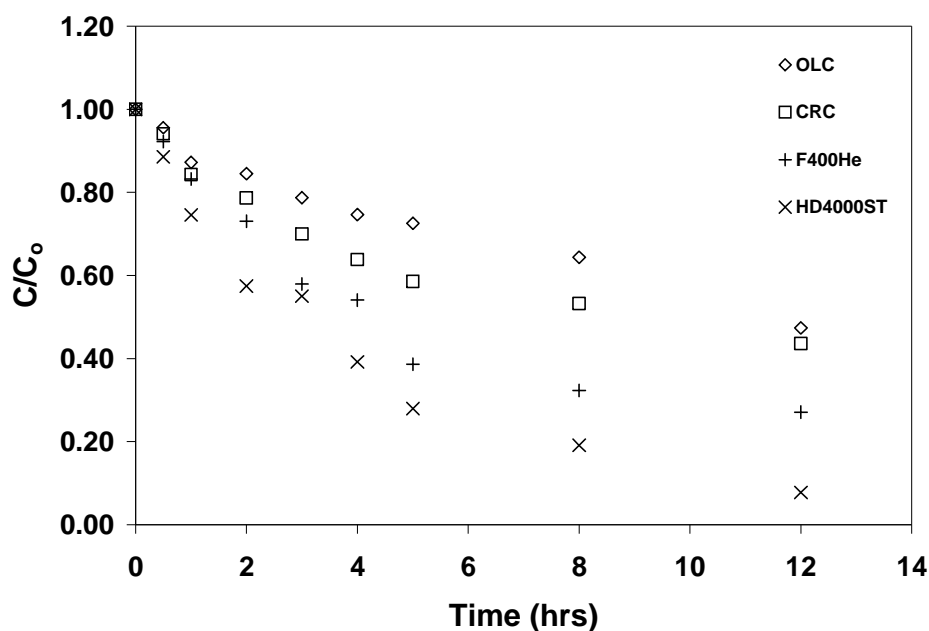


Figure 5.30 Atrazine adsorption kinetics in the presence of 5 mg DOC/L background DOM (twelve hours of contact time)

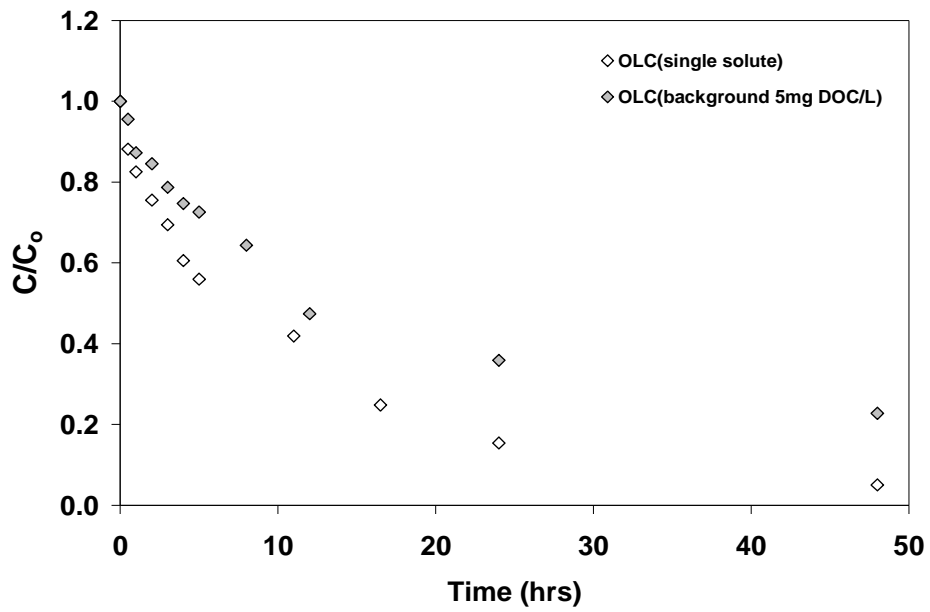


Figure 5.31 OLC adsorption kinetics for atrazine (two days of contact time)

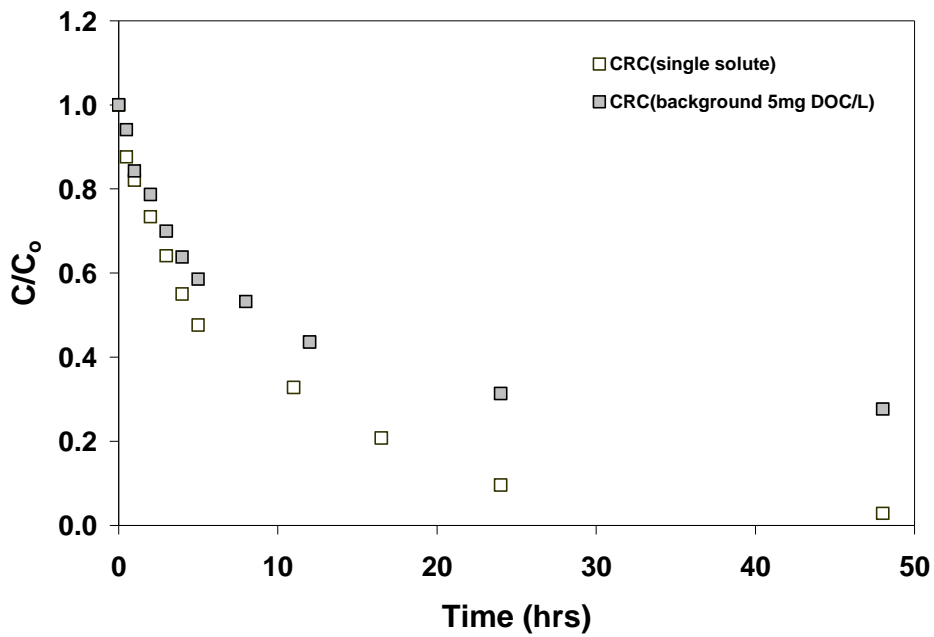


Figure 5.32 CRC adsorption kinetics for atrazine (two days of contact time)

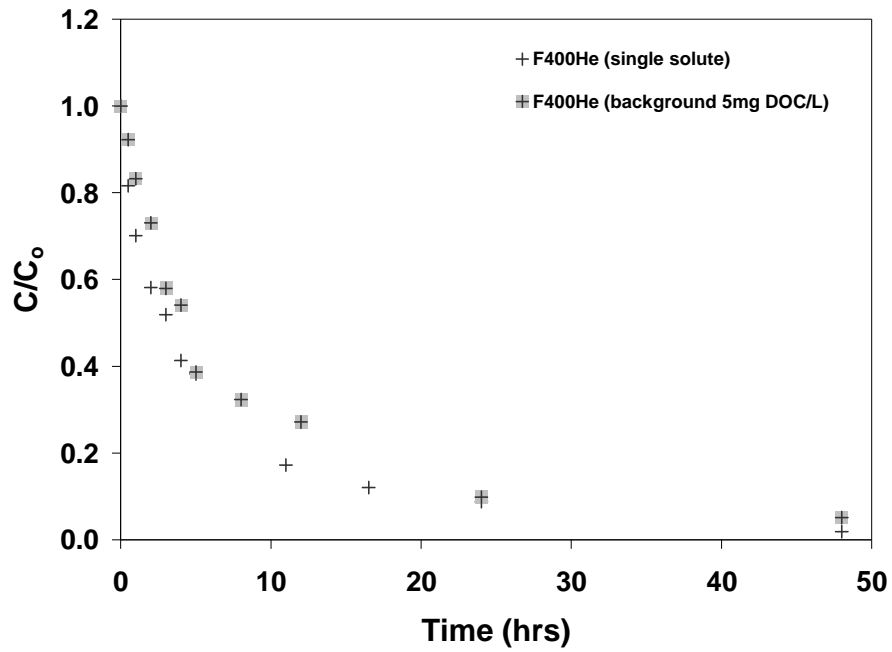


Figure 5.33 F400He adsorption kinetics for atrazine (two days of contact time)

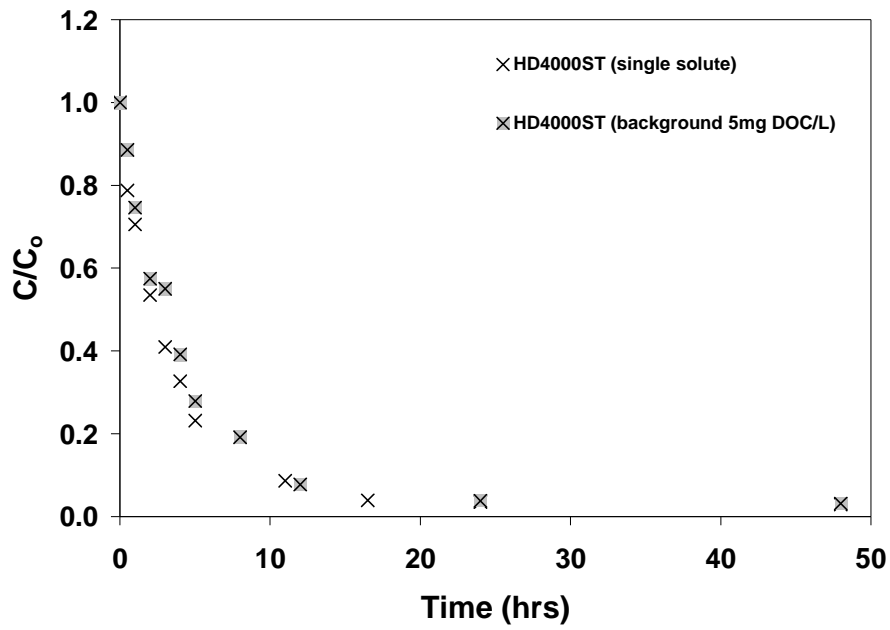


Figure 5.34 HD4000ST adsorption kinetics for atrazine (two days of contact time)



## CHAPTER 6

### CONCLUSIONS AND RECOMMENDATIONS

#### 6.1 Conclusions

Following major conclusions were obtained from this study:

- There exists a specific optimum adsorption pore size region for each micropollutant depending on its molecular dimensions. For example, TCE adsorbs in pores  $<10 \text{ \AA}$ , whereas atrazine adsorbs in pores  $10\text{-}20 \text{ \AA}$ . The removal of the SOC is enhanced with the increase in the volume in the specific pore size region. On the other hand, the components of the DOM used in this study did not adsorb in pores  $<10 \text{ \AA}$ .
- The relative relation between the optimum adsorption regions of the target SOC and background DOM determines the approach for selecting the GAC, and possibly the primary DOM competition mechanism on the adsorption of SOC by activated carbons. In this study, for TCE, the SOC with target adsorption region in the primary micropores which were inaccessible to DOM components, highly microporous carbons (i.e., having mainly pores less than  $10 \text{ \AA}$ ) showed the least DOM impact on the TCE adsorption. It appears that the highly microporous carbons acted as molecular sieves screening out the bulky DOM molecules and only allowing the access of TCE molecules to their target pore size region. It was found that DOM preloading effect was mainly due to pore blockage. For atrazine,

the SOC having a target adsorption region of 10-20 Å that overlaps with those of some DOM components, activated carbons with wider pore size distributions and high volumes in the target adsorption pore size region of the target SOCs demonstrated the lowest DOM preloading effect. The direct site competition was the primary DOM-SOC competition mechanism for atrazine adsorption.

- The results indicated that there are some pore structure properties (e.g., observations with the CRC and ACF10), which are not fully captured by the most commonly used carbon pore size distribution characterization techniques, that also exert some impact on the adsorption of SOC and DOM competition.
- Although performed in a limited number, the results of kinetics experiments showed that the mesoporous carbons have kinetic advantage over the microporous carbons for the competitive adsorption between SOC and DOM.

## 6.2 Recommendations for future research

The findings from this study are mainly based on the observations from isotherm experiments. These results should be further confirmed at representative drinking water conditions. For GAC fixed-bed adsorber applications, this can be accomplished by performing rapid small scale column tests (RSSCT) which have been shown to successfully predict the breakthrough of full scale columns. To capture long term preloading effects, the GAC in the RSSCT can be preloaded for different time periods prior to the target SOC adsorption.

The equilibrium experiments performed in this study used DOM collected from the influent to a drinking water treatment. Since the GAC fixed-bed adsorbers are located after conventional treatment processes which change the composition of DOM (i.e., high molecular weight components are preferentially removed), the RSSCTs should be performed using the water samples after conventional treatment processes.

For PAC applications, the contact time is usually short (0.5 – 2h), and the adsorption kinetics is critical during short contact times. Therefore, further kinetic investigations (e.g., using a typical jar test simulation PAC applications) should be performed to evaluate the extension of findings from this study to PAC applications.

Only two SOCs, TCE and atrazine, and one DOM were used in this study. Experiments need to be performed with more number of SOCs and DOMs in order to further generalize the findings obtained from this study.



## APPENDIX

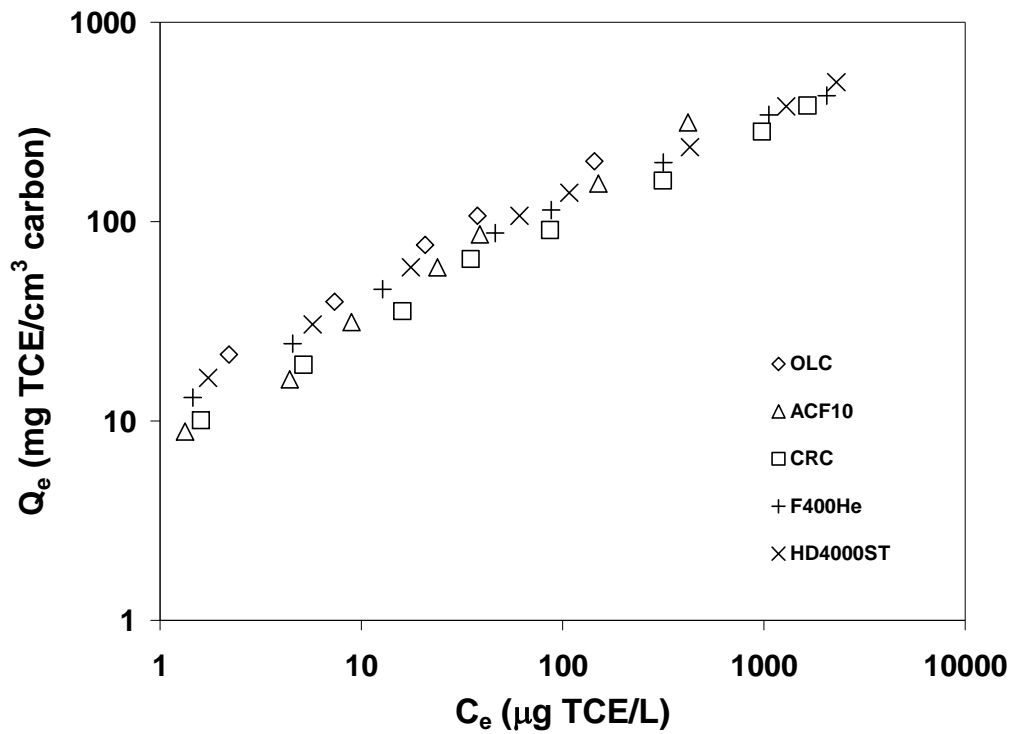


Figure A1: TCE adsorption isotherms in DDW normalized by volume available in 5-8 Å pore size region.

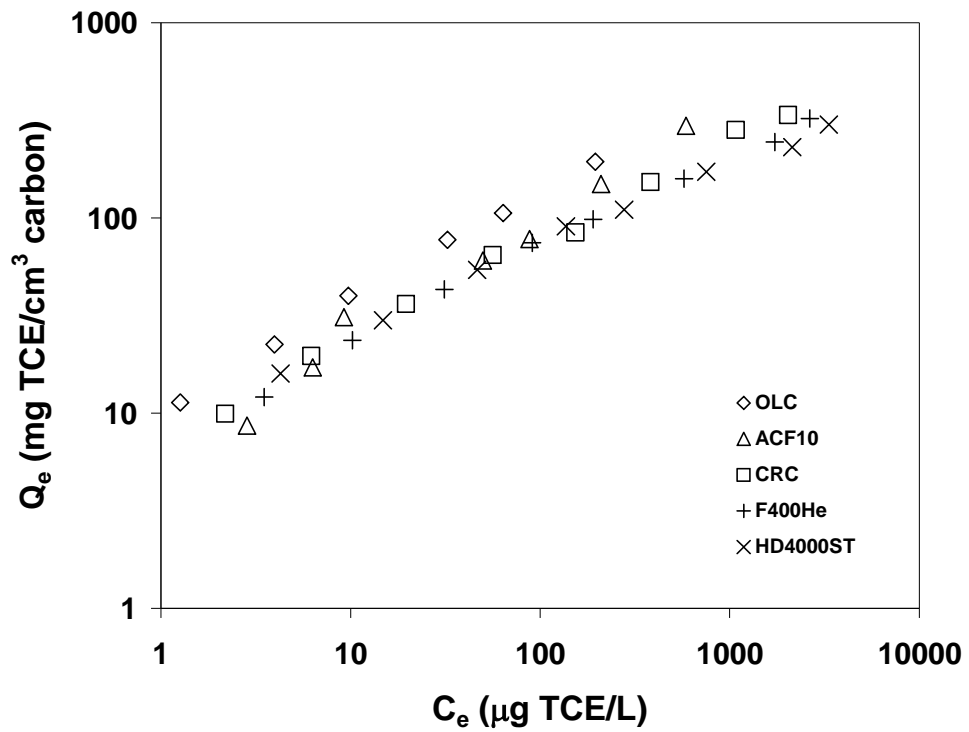


Figure A2: TCE adsorption for carbons preloaded by 5 mg/L DOM normalized by volume available in 5-8 Å pore size region.

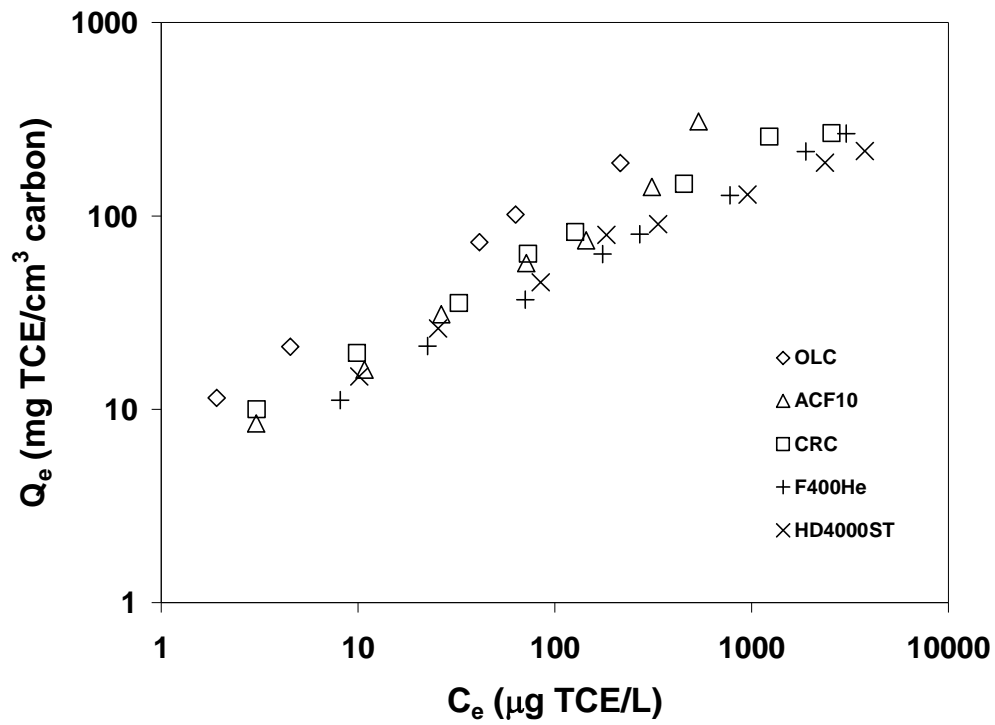


Figure A3: TCE adsorption for carbons preloaded with 20 mg/L DOM normalized by volume available in 5-8 Å pore size region.

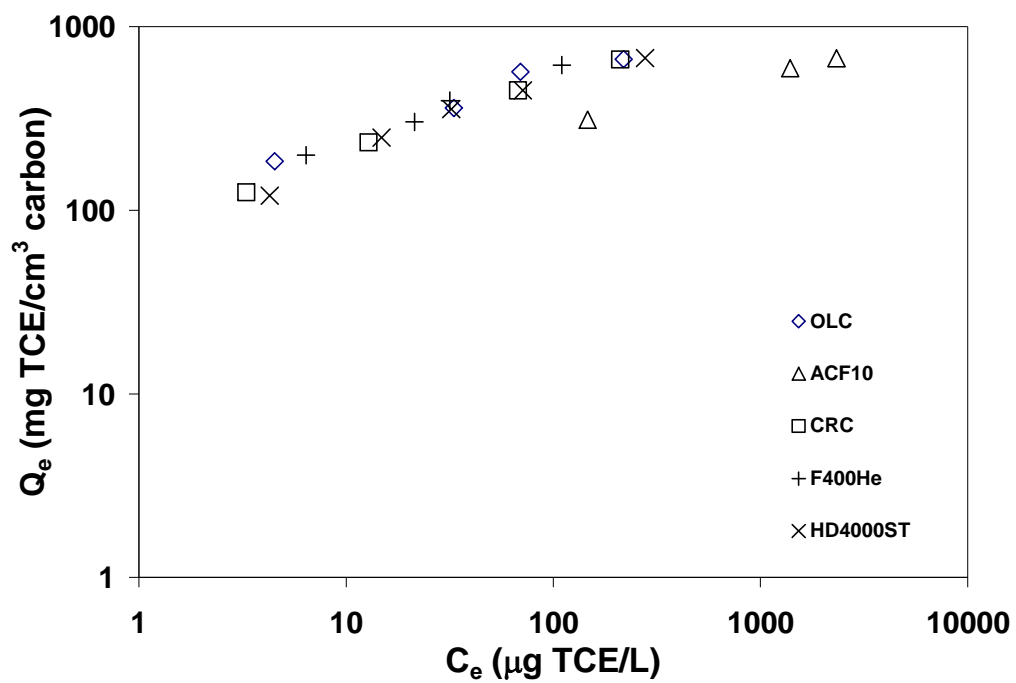


Figure A4: Atrazine adsorption isotherms for all carbons in DDW normalized by volume available in 10-20 Å pore size range.

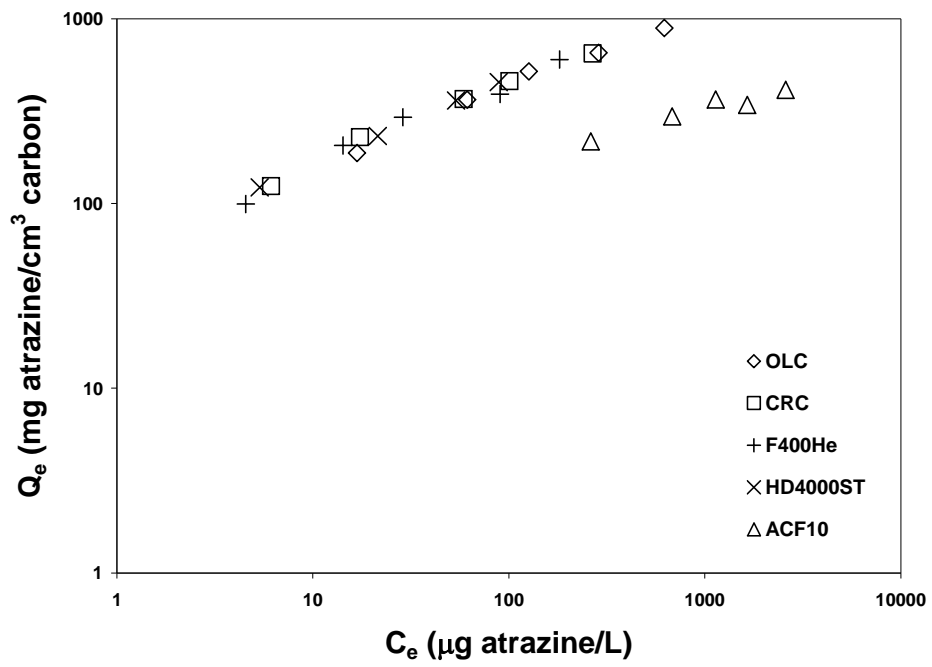


Figure A5: Atrazine adsorption isotherms for all carbons preloaded with 5 mg/L DOM normalized by volume available in 10-20 Å pore size region.

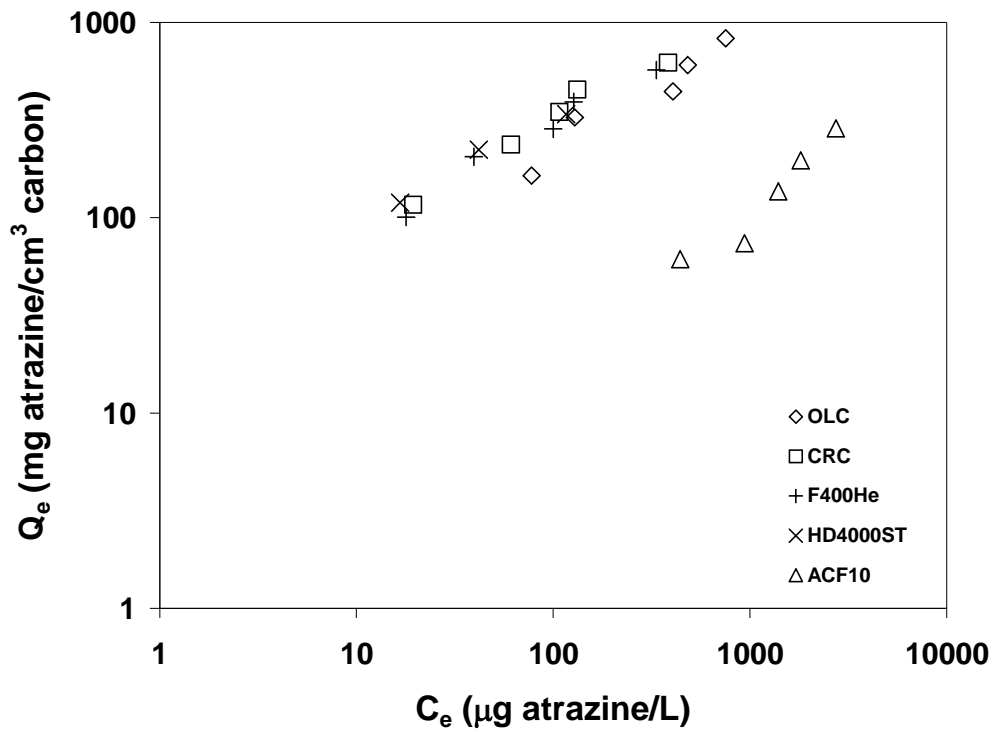


Figure A6: Atrazine adsorption isotherms for all carbons preloaded with 20 mg/L DOM normalized by volume available in 10-20 Å pore size region.

Table A1: Freundlich Coefficients for all TCE Adsorption Isotherms along with the 95% Confidence Intervals

| <b>Isotherm</b>                         | $K_F$ | <b>95%<br/>Confidence<br/>Interval</b> | $N$  | <b>95%<br/>Confidence<br/>Interval</b> |
|---|-------|--|------|--|
| <b>OLC</b> (single solute)              | 2.43  | 2.84 – 2.08                            | 0.57 | 0.62 – 0.52                            |
| <b>OLC</b> (preloading 5mg DOC/L)       | 1.97  | 2.20 – 1.76                            | 0.58 | 0.60 – 0.53                            |
| <b>OLC</b> (preloading 20mg DOC/L)      | 1.56  | 1.82 – 1.33                            | 0.59 | 0.63 – 0.55                            |
| <b>ACF10</b> (single solute)            | 1.78  | 2.24 – 1.42                            | 0.62 | 0.69 – 0.56                            |
| <b>ACF10</b> (preloading 5mg DOC/L)     | 1.30  | 1.96 – 0.86                            | 0.62 | 0.72 – 0.52                            |
| <b>ACF10</b> (preloading 20mg DOC/L)    | 0.78  | 1.33 – 0.51                            | 0.66 | 0.77 – 0.55                            |
| <b>CRC</b> (single solute)              | 1.79  | 2.11 – 1.51                            | 0.51 | 0.55 – 0.48                            |
| <b>CRC</b> (preloading 5mg DOC/L)       | 1.51  | 1.86 – 1.28                            | 0.51 | 0.55 – 0.47                            |
| <b>CRC</b> (preloading 20mg DOC/L)      | 1.32  | 1.71 – 0.82                            | 0.51 | 0.56 – 0.47                            |
| <b>F400He</b> (single solute)           | 2.10  | 2.48 – 1.56                            | 0.48 | 0.51 – 0.44                            |
| <b>F400He</b> (preloading 5mg DOC/L)    | 1.29  | 1.56 – 1.06                            | 0.48 | 0.51 – 0.44                            |
| <b>F400He</b> (preloading 20mg DOC/L)   | 0.66  | 0.74 – 0.58                            | 0.53 | 0.55 – 0.51                            |
| <b>HD4000ST</b> (single solute)         | 1.83  | 2.15 – 1.56                            | 0.47 | 0.50 – 0.44                            |
| <b>HD4000ST</b> (preloading 5mg DOC/L)  | 1.20  | 1.51 – 1.00                            | 0.44 | 0.47 – 0.39                            |
| <b>HD4000ST</b> (preloading 20mg DOC/L) | 0.78  | 1.10 – 0.56                            | 0.45 | 0.51 – 0.39                            |

## REFERENCES

- Baup, S.; Jaffre, C.; Wolbert, D. and Laplace, A. (2000). Adsorption of Pesticides onto Granular Activated Carbon: Determination of Surface Diffusivities Using Simple Batch Experiments. *Adsorption*, 6, 219-228.
- Bjelopavlic, M; Newcombe, G. and Hayes, R. (1999). Adsorption of NOM onto Activated Carbon: Effect of Surface Charge, Ionic Strength, and Pore Volume Distribution. *J. Colloid Interface Sci.* 210 (2), 271-280.
- Brunauer, S.; Emmett, P.H. and Teller, E. (1938). Adsorption of Gases in Multimolecular Layers. *J. Phys. Chem.* 60, 309–319.
- Cal M.P., Larson S.M. and Rood M.J. (1994). Experimental and Modeled Results Describing the Adsorption of Acetone and Benzene onto Activated Carbon Fibers, *Env. Prog.*, 1994, 13 (1), 26.
- Carter, M.C.; Weber, W.J.Jr. and Olmstead, K.P. (1992). Effects of Background Dissolved Organic Matter on TCE Adsorption by GAC. *J.AWWA*, 84, 8, 81-91.
- CRC Handbook of Chemistry and Physics, 73<sup>rd</sup> edition, Lide, D.R., Ed.; CRC Press, 1992-1993, 15-48.
- Croue, J. P.; Benedetti, M. F.; Violleau, D. and Leenheer, J. A. (2003). Characterisation and Copper Binding of Humic and Nonhumic Matter Isolated From The South Palette River: Evidence for the Presence of Nitrogenous Binding Sites. 37(2), 328-336.
- Dastgheib, S.; Cheng, W. and Karanfil, T. (2004). Tailoring Activated Carbons for Enhanced Removal of Natural Organic Matter from Natural Waters. *Carbon* 43, 3, 547-557
- Dimotakis, E.D.; Cal, M.P.; Economy, J.; Rood, M.J. and Larson, S.M. (1995). Chemically Treated Activated Carbon Cloths for Removal of Volatile Organic Carbons from Gas Streams: Evidence for Enhanced Physical Adsorption. *Environ. Sci. Technol.*, 29, 1876-1880.
- Dubinin, M.M. and Radushkevich, L. V., (1947). Equation of the Characteristic Curve of Activated Charcoal. *Proc. Acad. Sci. USSR*, 55, 331.

- Ebie, K.; Li, F.; Azuma, Y.; Yuasa, A. And Hagishita, T. (2000). Pore Distribution Effect of Activated Carbon in Adsorbing Organic Micropollutants from Natural Water. *Wat. Res*, 35 (1), 167-179.
- Economy, J.; Foster, K.; Andreopoulos, A. and Jung, H. (1992). Tailoring Carbon Fibers for Adsorbing Volatiles. *Chemtech*, 597-603.
- Electronics Cooling, [http://electronics-cooling.com/html/2001\\_august\\_techbrief.html](http://electronics-cooling.com/html/2001_august_techbrief.html), 2007.
- Everett, H.D. and Powl, J.C. (1976). Adsorption in Slit-like and Cylindrical Micropores in the Henry's Law Region, *J. Chem. Soc., Faraday Trans. 1*, 72, 619–636.
- Foster, K. L.; Fuerman, R.G.; Economy, J.; Larson, S. M.; and Rood, M. J. (1992). Adsorption Characteristics of Trace Volatile Organic Compounds in Gas Streams onto Activated Carbon Fibers. *Chem. Mater.*, 4(5), 1068-73.
- Freeman, J. J.; Gimblett, F. R. G. and Sing, K. S. W. (1989). Studies of Activated Charcoal Cloth. V. Modification of Pore Structure by Impregnation with Certain Transition Metal salts and Oxo-Complexes. *Carbon*, 27, 85-93.
- Greg, J. and Sing, K.S.W. (1982). In *Adsorption Surface Science and Porosity*, 2<sup>nd</sup> ed. Academic Press, London. p.200
- Halfon, E. (1985). Regression Method in Ecotoxicology: A Better Formation Using the Geometric Mean Functional Regression. *Environ. Sci. Technol.* 19(8) 747.
- Hayes, J.S. (1985). Novoloid Nonwovens. *Nonwoven Symposium*, 257-263. TAPPI Press.
- Hopman, R.; Siegers, W. G. and Kruithof J. C. (1995). Organic Micropollutant Removal by Activated Carbon Fiber Filtration. *Water Supply*, 13, 257-261.
- Jagtoyen, M. and Derbyshire, F. J. (1993). Some Considerations of the Origins of Porosity in Carbons from Chemically Activated Wood. *Carbon* 31, 1185-1192.
- Jagtoyen, M.; Thwaites, M.; Stencil, J.; McEnaney, B. and Derbyshire, F. J. (1992). Adsorbent Carbon Synthesis from Coals by Phosphoric Acid Activation. *Carbon*, 30, 1089-96.
- Jankowska, H.; Swiatkowski, A.; Starostin, L. and Tawrinienko-Omicynska, J. (1991). Adsorption of Ions on Activated Carbon, PWN, Warsaw, 1991 (in Polish).

- Kaneko, K.; Setoyama, N.; Suzuki, T. and Kuwabara, H. (1993). Ultramicroporosity of Porous Solids by He Adsorption. Proceedings of the Fourth International Conference on Fundamentals of Adsorption, International Adsorption Society, Boston.
- Karanfil, T., (2006). Activated Carbon Adsorption in Drinking Water Treatment. In: Activated Carbon Surfaces in Environmental Remediation, Bandosz, T.J (Ed).
- Karanfil, T. and Dastgheib, S.A. (2004). Trichloroethylene Adsorption by Fibrous and Granular Activated Carbons: Aqueous Phase, Gas Phase and Water Vapor Adsorption Studies. Environ. Sci. Technol., 38(22), 5834-5841.
- Karanfil, T. ; Dastgheib, S.A.; Mauldin D. (2006). Exploring Molecular Sieve Capabilities of Activated Carbon Fibers to Reduce the Impact of NOM Preloading on Trichloroethylene Adsorption. Environ. Sci. Technol., 40(4) 1321-1327.
- Karanfil, T. and Kilduff, J. E. (1999). Role of Granular Activated Carbon Surface Chemistry on the Adsorption of Organic Compounds. 1. Priority Pollutants. Environ. Sci. Technol., 33, 3217-3224.
- Karanfil, T.; Kilduff, J. E.; Schlautman, M.A. and Weber, W.J. Jr. (1998). Oxygen Sensitive Sorption of Natural and Synthetic Organic Macromolecules by GAC: Effect of Solution chemistry. Water Res., 32, 154-164.
- Kasaoka, S.; Sakata, Y.; Tanaka, E. and Naitoh, R. (1989a). Preparation of Activated Fibrous Carbon from Phenolic Fabric and its Molecular Sieve Properties. Int. Chem. Eng., 29, 101-104.
- Kasaoka, S.; Sakata, Y.; Tanaka, E. and Naitoh, R. (1989b). Design of Molecular Sieve Carbon. Studies on the Adsorption of Various Dyes in the Liquid Phase. Int. Chem. Eng., 29, 734-742.
- Kilduff, J.E. and Karanfil, T. (2002). Trichloroethylene Adsorption by Activated Carbon Preloaded with Humic Substances: Effects of Solution Chemistry. Wat Res. 36, 1685-1698.
- Kilduff, J.E; Karanfil, T. and Chin, Y. P. (1996). Adsorption of Natural Organic Polyelectrolytes by Activated Carbon: A Size-Exclusion Chromatography Study. Environ. Sci. Technol. 30, 1336-1343.
- Kilduff, J.E.; Srivastava, R. and Karanfil, T. (2002). Stud. Surf. Sci. Catal., 553.

- Kitis, M. Kilduff, J. E; Kaaranfil, T. (2001). Isolation of Dissolved Organic Matter from Surface Waters Using Reverse Osmosis and its Impact on the Subsequent Reactivity of DOM to Formation and Speciation of Disinfection By-Products. *Wat. Res* (2001), 35, 9, 2225-2234
- Lalezary, S.; Pirbazari, M.; McGuire, M. (1986). Evaluating Activated Carbons for Removing Low Concentrations of Taste and Odor producing Organics. *J. AWWA*, 78, 11, 76-82.
- Lastoskie, C; Gubbins, K.E and Quireke, N. (1993). Pore Size Heterogeneity and the Carbon Slit Pore: A Density Functional Theory Model. *Langmuir*, 9, 2693-2702.
- Lee, M. C.; Snoeyink, V.L. and Crittenden, J.C. (1981). Activated Carbon Adsorption of Humic Substances. *J. AWWA*, 73, 440-446.
- Mangun, L.C.; Benak, R. K.; Economy, J. and Foster, L. K. (2001). Surface Chemistry, Pore Size and Adsorption Properties of Activated Carbon Fibers and Precursors Treated with Ammonia. *Carbon*, 39, 1809-1820.
- Mangun, L.C.; Benak, R.K.; Daley, A. M. and Economy, J. (1999). Oxidation of Activated Carbon Fibers: Effect on Pore Size, Surface Chemistry and Adsorption Properties. *Chem. Mater.*, 11, 3476-3483.
- Matsui, Y.; Knappe, D.R.U. and Takagi, R. (2002). Pesticide Adsorption by Granular Activated Carbon Adsorbers.1. Effect of Natural Organic Matter Preloading on Removal Rates and Model Simplification. *Environ. Sci. Technol*, 36, 3426-3431.
- McGuire, M.J.; McLain, J.L.; Obolensky, A. (2002) Information Collection Rule Data Analysis. American Water Works Assosiation Research Foundation Report, Denver, Colorado, 2002.
- Moore, B.C.; Cannon, F.S.; Westrick, J.A.; Metz, D.H.; hrive, C.A.; DeMarco, J.and Hartmen, D.J. (2001) Changes in GAC pore structure during full-scale water treatment at Cincinnati: a comparison between virgin and thermally reactivated GAC. *Carbon*, 39, 789-807.
- Mowla, D.; Do, D.D.; Kaneko, K. (2003). Adsorption of Water Vapor in Activated Carbon: A Brief Review. *Chemistry and Physics of Carbon*, 28, 229-262, 2003.
- Najim, I. N.; Snoeyink, V. L.; Suidan, M.; Lee, C.H; Richard, Y.; (1990) Effet of Particle Size and Background Natural Organics on the Adsorption Efficiency of PAC. *J. AWWA.*, 82, 1, 65-72.

- Newcombe, G. (1999). Charge vs. Porosity - Some Influences on the Adsorption of Natural Organic Matter (NOM) by Activated Carbon. *Water . Sci. Tech.* 40 (9) 191-198.
- Newcombe, G. and Drikas, M. (1997). Adsorption of NOM onto Activated Carbon: Electrostatic and Non-Electrostatic Effects. *Carbon*, 1239-1250.
- Newcombe, G.; Drikas, M. and Hayes, R. (1997). Influence of Characterized Natural Organic Material on Activated Carbon Adsorption: II Effect of Pore Volume Distribution and Adsorption of 2-Methylisoborneol. *Water Res.*, 31, 1065-1073.
- Newcombe, G.; Morrison, J.; Hepplewhite, C. and Knappe, D.R.U. (2002) Simultaneous Adsorption of MIB and NOM onto Activated Carbon II. Competitive Effects. *Carbon* (40) 2147-2156.
- Olmstead, K. P. and Weber, W. J. Jr. (1990). Statistical Analysis of Mass Transfer Parameters for Sorption Processes and Models. *Environ. Sci. Technol.* 24(11), 1693.
- Pan, D. and Jaroniec, M. (1996). Adsorption and Thermogravimetric Studies of Unmodified and Oxidized Active Carbons. *Langmuir*, 3657-65.
- Pelekani, C.; Snoeyink, V. L. (1999). Competitive Adsorption in Natural Water: Role of Activated Carbon Pore Size. *Wat. Res*, 33 (5), 1209-1219.
- Pelekani, C.; Snoeyink, V. L. (2000). Competitive Adsorption Between Atrazine and Methylene Blue on Activated Carbon: The Importance of Pore Size Distribution. *Carbon* 38(2000) 1423-1436.
- Pelekani, C.; Snoeyink, V. L. (2001) A Kinetic and Equilibrium Study of Competitive Adsorption between Congo Red Dye on Activated Carbon: The Importance of Pore Size Distribution. *Carbon* 39(2001) 25-37.
- Polanyi, M. (1914). *Verb. Deutsch. Physik. Ges.*, 16, 1012.
- Pontius, F.W. (1996a). An Update of the Federal Regulations. *J. Am. Water Works Assoc*, 88(3), 36.
- Pontius, F.W. (1996b). Inside the Information Collection Rule. *J. Am. Water Works Assoc*, 88(8), 16.
- Puri, B. R. (1970). *Chemistry and Physics of Carbon*. Vol. 6, Walker, P. L. Jr. (Ed.). Marcel Dekker Inc.: New York.

- Quinlivan, P. A.; Li Lei; Knappe, D. R. U. (2005). Effects of Activated Carbon Characteristics on the simultaneous Adsorption of Aqueous Organic Micropollutants and Natural Organic Matter. *Water Research*, 39, 1663-1673.
- Radovic, L. R.; Moreno-Castilla, C. and Rivera-Utrilla, J. (1997). *Chemistry and Physics of Carbon*. Vol 26, Thrower, P.A. and Radovic L. R. (Eds.). Marcel Dekker.
- Ross, S. and Morrison, I. D. (1988). *Colloidal Systems & Interfaces*, Wiley-Interscience, New York.
- Schwarzenbach, R. P.; Gschwend, P. M.; Imboden, D. M. (2003). *Environmental Organic Chemistry*, second edition. John Wiley & sons, inc., publications.
- Smith, E. H. and Weber, W. J. Jr. (1989). Evaluation of Mass Transfer Parameters for Adsorption of Organic Compounds from Complex Organic Matrices. *Environ. Sci. Technol*, 23(6), 713-722.
- Snoeyink, V. L. and Weber, W. J. Jr. (1967). The Surface Chemistry of Active Carbon: Discussion of Structure and Surface Functional Groups. *Environ. Sci. Technol*, 1(3), 228.
- Solum, M. S.; Pugmire, R. J.; Jagtoyen, M. and Derbyshire, F. J. (1995). Evolution of Carbon Structure in Chemically Activated Wood. *Carbon*, 33, 1247-54.
- Summers, R. S; Haist, B.; Koehler, J.; Ritz, J.; Sontheimer, H. (1989) The Influence of Background Organic Matter on GAC Adsorption. *J. AWWA*. 81, 5, 66-74.
- Summers, R.S. and Roberts, P.V. (1988a). Activated Carbon Adsorption of Humic Substances: I. Heterodisperse Mixtures and Desorption. *J. Colloid and Interface Science*, 122, 367-381.
- Summers, R.S. and Roberts, P.V. (1988b). Activated Carbon Adsorption of Humic Substances: II Size Exclusion and Electrostatic Interactions. *J. of Colloid and Interface Science*, 122, 382-397.
- Thurman, E. M. *Organic Geochemistry of Natural Waters*, Martinus Nijhoff-Dr. Junk Publishers, Dordrecht, The Netherlands, 1985.
- USEPA Regulatory Agenda. Notice. Federal Register. (1995). 60:228:60610, November 28, 1995.
- USEPA. Safe Drinking Water Act, <http://www.epa.gov/safewater/sdwa/index.html>, 2007.

- Webb, A.P. and Orr, C. (1997). Surface Area and Pore Structure by Gas Adsorption. In: Analytical Methods in Fine Particle Technology, 54-153, Camp, R.W.; Olivier, J. P. and Yunes, Y. S. (Eds.). Micromeritics Instrument Corporation, Norcross, GA.
- Weber, W.J. Jr. (1972). Physicochemical Processes for Water Quality Control. New York: Wiley-Interscience.
- Weber, W. J. Jr. and Pirazari M. (1982). Adsorption of Toxic and Carcinogenic Compounds from Water. J. AWWA, 74, 203.
- Weber, W. J. Jr. and Van Vliet, M. B. (1980). Fundamental Concepts for Application of Activated Carbon in Water and Wastewater Treatment. In: Activated Carbon Adsorption of Organics from Aqueous Phase, vol.1, Suffet, H. I. and McGuire, J. M. (Eds.).
- Wolff, W.F. (1959). A Model of Active Carbon. J. Phys. Chem., 63,653.
- Yang, R. T. (1984). Etch-decoration Electron Microscopy Studies of Gas-Carbon Reactions. In: Chemistry and Physics of Carbon, vol. 19, Thrower, P. A., (Ed.). Dekker, New York, NY.
- Yang, R. T. and Duan, R. Z. (1985). Kinetics and Mechanism of Gas-Carbon Reactions: Conformation of Etch Pits, Hydrogen Inhibition and Anisotropy in Reactivity. Carbon 23, 325-331.